DEFENSE TECHNICAL INFORMATION CENTER

Information for the Defense Community

DTIC® has determined on 6/13/12 that this Technical Document has the Distribution Statement checked below. The current distribution for this document can be found in the DTIC® Technical Report Database.

☒ **DISTRIBUTION STATEMENT A.** Approved for public release; distribution is unlimited.

☐ **© COPYRIGHTED.** U.S. Government or Federal Rights License. All other rights and uses except those permitted by copyright law are reserved by the copyright owner.

☐ **DISTRIBUTION STATEMENT B.** Distribution authorized to U.S. Government agencies only (fill in reason) (date of determination). Other requests for this document shall be referred to (insert controlling DoD office).

☐ **DISTRIBUTION STATEMENT C.** Distribution authorized to U.S. Government Agencies and their contractors (fill in reason) (date determination). Other requests for this document shall be referred to (insert controlling DoD office).

☐ **DISTRIBUTION STATEMENT D.** Distribution authorized to the Department of Defense and U.S. DoD contractors only (fill in reason) (date of determination). Other requests shall be referred to (insert controlling DoD office).

☐ **DISTRIBUTION STATEMENT E.** Distribution authorized to DoD Components only (fill in reason) (date of determination). Other requests shall be referred to (insert controlling DoD office).

☐ **DISTRIBUTION STATEMENT F.** Further dissemination only as directed by (insert controlling DoD office) (date of determination) or higher DoD authority.

Distribution Statement F is also used when a document does not contain a distribution statement and no distribution statement can be determined.

☐ **DISTRIBUTION STATEMENT X.** Distribution authorized to U.S. Government Agencies and private individuals or enterprises eligible to obtain export-controlled technical data in accordance with DoDD 5230.25; (date of determination). DoD Controlling Office is (insert controlling DoD office).

REPORT DOCUMENTATION PAGE

Form Approved
OMB No. 0704-0188

1. REPORT DATE *(DD-MM-YYYY)*	2. REPORT TYPE	3. OATES COVERED *(From - To)*
19-03-2012	Final	14 Sept 2009 - 13 March 2012

4. TITLE AND SUBTITLE
Final Report - Blood biomarkers for assessing the exposure and response of mammals to chemical and biological agents

5a. CONTRACT NUMBER
W911SR-09-C-0062

5b. GRANT NUMBER

5c. PROGRAM ELEMENT NUMBER

6. AUTHOR(S)
Hood, Leroy; Lausted, Christopher; Glusman, Gustavo; Rowen, Lee; Wang, Kai; Hu, Zhiyuan

5d. PROJECT NUMBER

5e. TASK NUMBER

5f. WORK UNIT NUMBER

7. PERFORMING ORGANIZATION NAME(S) AND ADDRESS(ES)
Institute for Systems Biology
401 Terry Avenue North
Seattle, WA 98109-5234

8. PERFORMING ORGANIZATION REPORT NUMBER

9. SPONSORING/MONITORING AGENCY NAME(S) AND ADDRESS(ES)
DCMA Seattle - S4801A
Corporate Campus East 111
3009 112th Ave NE Suite 200
Bellevue, WA 98001-8019

10. SPONSOR/MONITOR'S ACRONYM(S)
DCMA

11. SPONSORING/MONITORING AGENCY REPORT NUMBER

12. DISTRIBUTION AVAILABILITY STATEMENT
See Section H: H.1 Worldwide Web Restrictions H.2 Release of information. H.4.1 Written approval from CO required to employ foreign nationals in the performance of said contract.

13. SUPPLEMENTARY NOTES

14. ABSTRACT
We aimed to develop strategies for performing quantitative analyses of organ-specific blood biomarkers by: 1) developing better software for analyzing dynamically changing transcriptomes; 2) analyzing blood and multiple organs/tissues of animals from three inbred mouse strains exposed to the toxins acetaminophen and carbon tetrachloride for transcriptomes, proteins and miRNA biomarkers.; 3) establishing MRM mass spectrometry assays for at least 25 liver-specific blood proteins based on the acetaminophen, CCL4, and other model systems of interest; 4) analyzing blood and tissue of animals from three inbred mouse strains exposed to the toxins acetaminophen and carbon tetrachloride for protein biomarkers using proteomics technologies, including MRM; 5) Analyzing time course experiments of rat tissues and blood exposed to VX; and 6) Developing new technologies for developing protein-capture agents and the analyses of single protein molecules. Although discovery and validation of organ-specific biomarkers are challenging from a technical perspective, we made considerable progress towards achieving our stated aims.

15. SUBJECT TERMS
Blood Biomarkers, software development, protein capture agents, single protein molecules.

16. SECURITY CLASSIFICATION OF:			17. LIMITATION OF ABSTRACT	18. NUMBER OF PAGES	19a. NAME OF RESPONSIBLE PERSON
a. REPORT	b. ABSTRACT	c. THIS PAGE			Trudy Adkins
UU	UU	UU	UU	45	19b. TELEPONE NUMBER *(Include area code)* 206-732-1222

20120418053

A. COVER SHEET

Contractor's Final Report

Contractor name and address:	Institute for Systems Biology 401 Terry Ave N Seattle WA 98109
Contract Number:	W911SR-09-C-0062
Project Name:	BAA, Blood biomarkers for assessing the exposure and responses of mammals to chemical and biological agents
Report Date:	March 15, 2012
Period Covered:	September 14, 2009-March 15, 2012
Report Title:	Scientific and technical final comprehensive report_ISB
Security classification:	Unclassified
Issuing Government Activity:	US ARMY RDECOM ACQ CTR -W911SR EDGEWOOD CONTRACTING DIVISION AMSRD-ACC-E/BLDG E4455 E5179 HOADLEY ROAD ABERDEEN PROVING GROUND MD 21010-5401

Scientific and technical report
Final Comprehensive Report

B. Description of progress made against milestones during the reporting period

Our blood biomarker proposal had several specific objectives and aims, listed here:
Aim 1: Develop better software for analyzing dynamically changing transcriptomes.
Aim 2: Analyze the bloods and multiple organs/tissues of animals from three inbred mouse strains exposed to the toxins acetaminophen and carbon tetrachloride for transcriptomes, proteins and miRNA biomarkers.
Aim 3: Establish MRM mass spectrometry assays for at least 25 liver-specific blood proteins based on the acetaminophen, CCL4, and other model systems of interest.
Aim 4: Analyze the bloods and tissues of animals from three inbred mouse strains exposed to the toxins acetaminophen and carbon tetrachloride for protein biomarkers using proteomics technologies, including MRM.
Aim 5: Analyze time course experiments of rat tissues and blood exposed to VX.
Aim 6: Develop new technologies for developing protein-capture agents and the analyses of single protein molecules.

Summary

At ISB, we have conducted research related to these aims over the past several years. Our results and conclusions are presented here. The discovery and validation of organ-specific biomarkers are challenging from a technical perspective. Nonetheless, we have made considerable progress and, along with the 4 papers already published on our work (see below), we anticipate that at least four additional manuscripts will be written and submitted for publication within the next few weeks or months. Two invention applications have been filed with the patent office. Planned and actual publications and invention disclosures are listed in the appropriate research descriptions.

Progress made with respect to the specific aims

Transcriptome analysis software

Aim 1: Develop better software for analyzing dynamically changing transcriptomes.

Two approaches were taken to this aim. In the first approach (A), a standard RNASeq analysis pipeline for standard transcriptomic experiments was constructed by Victor Cassen. A second, more sophisticated approach conducted by Gustavo Glusman (B), describes in detail how best to normalize, or scale, transcriptome data.

A. Development of a pipeline for processing RNASeq data

RNA-Seq is a technology that is gaining popularity due to its high utility, sensitivity, and reliability, while simultaneously benefitting from continually reduced costs. However, with the rapid rise in data volumes generated by RNASeq and other high throughput sequencing technologies, new challenges in data management and analysis have arisen.

The RNASeq pipeline is a software package designed to aid in the computational analysis of RNASeq data. Rather than embrace a single approach, the pipeline is designed to facilitate the running of multiple, separately written analysis software

programs that together constitute a meaningful analysis of the data at hand. This approach offers several benefits relating to flexibility:

- Different projects will have different needs; a project that is interested primarily in identifying differential gene expression (e.g., to quantify networks) may not be interested in novel alternative splicing discovery. However, various steps (e.g., filtering) may still be common to both processing pipelines. The RNASeq pipeline allows the user to easily incorporate common software steps into various pipelines, abetting software re-use.

- As analysis algorithms are continuously refined, replaced, and superceded, they can be swapped in and out of the RNASeq pipeline with relative ease. Additionally, algorithms can easily and reproducibly be compared, both against themselves (e.g., with different parameter values) or against other algorithms. The RNASeq pipeline incorporates a provenance database that records all the information needed to reproduce a pipeline run, as well as performance statistics.

Features of the software:

- A collection of pre-configured pipelines and pipeline steps to handle common RNASeq processing tasks.
- Support for a variety of input data types, including single and paired end data.
- Sun Grid Engine (SGE) support allows pipelines to be run on clusters for enhanced performance.
- Recording of all pipeline runs, including reproduction and performance data.
- Pipeline run reports.

Methodology:

The RNASeq pipeline works by combining the inputs of three configuration files per run to produce a unix-based shell script that can be run on a user's local desktop or submitted to an SGE cluster. The three inputs correspond to 1) a description of the read data to be processed, including it's location on the host's filesystem; 2) a description of the pipeline to be applied to the data; and 3) a site-wide configuration file containing information pertinent to host. The resulting shell script incorporates commands for each step specified in the pipeline's configuration file, matching the outputs of various steps to the inputs of dependent steps as directed. Interspersed with the commands for each step are calls to RNASeq pipeline-specific commands that record the results and execution times of each step into a per-user data, which is then later used to generate run reports.

Documentation:

A webpage describing the installation and use of the pipeline may be found at http://vcassen.gdxbase.org/RNA-Seq

B. Analysis of digital transcriptomes: optimal scaling and identification of tissue-specific genes (Gustavo Glusman reporting)

Conceptual overview: We have developed a comprehensive transcriptomics analysis pipeline focusing on digital transcriptomics data (MPSS, RNASseq). The analysis pipeline links a series of computational tasks, as shown in Figure 1.

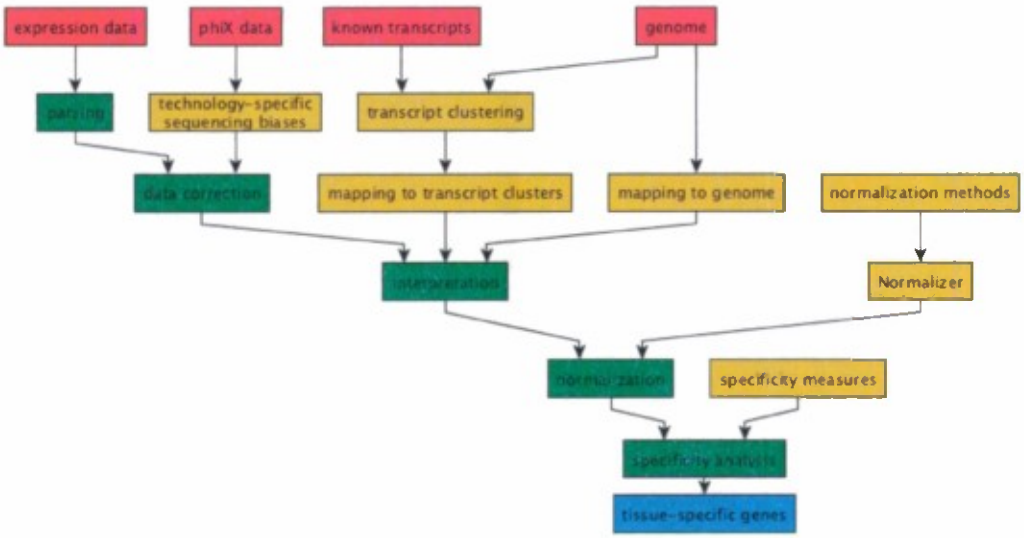

Figure 1. Starting from the expression data sets, known transcripts and the genome reference (red boxes), a series of computational tasks (green boxes) lead to the identification of tissue-specific genes (blue). These tasks are supported by a variety of additional computational procedures (yellow).

We developed a variety of tools for performing the preliminary data management and transformation procedures. Parsing and data correction methods are naturally technology-specific. Proper interpretation of the observed sequence reads via mapping to transcript clusters and to the genome is crucial for avoiding both false negatives (by discarding or mismapping reads) and false positives (by mismapping reads or by giving credence to ambiguous mapping results). Nevertheless, while these potential failures can lead to errors in establishing the relative expression levels of different genes, they are largely consistent when evaluating the expression level of each gene, in different samples. Conversely, proper performance of the data normalization task is crucial in preparation for cross-sample comparisons of gene expression levels. These latter comparisons are the core and central concept on which the identification of tissue-specific genes is based. We therefore spent significant effort studying and perfecting methods for accurate data normalization via scaling algorithms.

Methods for normalization: In contrast to methods based on hybridization, in digital transcript counting the observed absolute expression level of each gene and transcript will depend on the depth to which each sample was sequenced: deeper sequencing will uncover transcripts expressed at very low levels, and will proportionally increase the observed expression levels of more prevalent transcripts.

Many data standardization methods have been proposed to date, most frequently by scaling the values observed in each sample. The most commonly used method normalizes expression values to the total number of reads observed in each sample: gene expression values are thus expressed in terms of "counts per million" (CPM) or "transcripts per million" (TPM); for RNASeq, the equivalent measure is "reads per kb per million" (RPKM). This method has the advantage of simplicity as samples can be normalized independently, but its results are sensitive to highly expressed genes: since much sequencing output is spent on the most prevalent genes, the presence of a few, highly-expressed tissue-specific genes can significantly lower the CPM values for all other genes, often leading to the wrong conclusion that the latter are "down-regulated".

A way to avoid such distortions is to normalize gene counts in terms of quantiles; the median expression value as commonly used for normalization of microarray data. Due to the preponderance of zero and low-count genes in digital transcriptomes, the median value is usually uninformative, but expression values may be scaled based on the upper quartile. Alternatively, it is possible to adjust the overall expression levels of all genes so that the distributions for all samples become equalized. This method cancels global biases but, since it does not rely on scaling, it distorts the pairwise gene expression ratios within each sample.

A different class of normalization methods relies on the expression level of a subset of the genes to "guide" the normalization. At its simplest level, one may assume that the expression levels of certain "housekeeping" genes (e.g., *GAPDH*, *HPRT*) are constant across cell types, and can therefore be used individually as an internal normalization tool. This assumption has been shown to be invalid in various scenarios, leading to incorrect results. More elaborate methods therefore rely on minimizing the variance of not just one, but a small set of guide genes, or consider the relative RNA production of pairs of samples, under the assumption that the majority of genes are not differentially expressed.

We implemented a large number of existing normalization methods and some variations on them, and also devised entirely different approaches to data normalization. We encapsulated all these methods in an open-source, portable Perl module and an equivalent R package.

Classification and structure of normalization methods: We identified a small number of core concepts on which the many normalization methods are based. With the single exception of the Quantile Normalization method, all the algorithms we considered are global procedures that scale all the values in each sample using a single "scaling factor" (Figure 2, next page). Some of the scaling methods are *based on a global characteristic of each sample* (Fig. 2, left), i.e., they study each sample independently and identify a characteristic value used for normalization. This characteristic value can be the sum of all counts (CPM method), or a specific expression level, e.g., at the upper quartile. We added two variations on these methods: using total counts but scaling samples relative to each other ("Total" method), and scaling to the upper decile.

Alternatively, some scaling methods are *based on pre-selected genes* (Fig. 2, right), either using the expression value of a single housekeeping gene to guide normalization, or selecting the subset of housekeeping genes that are most consistent with each other ("most stable") and using the geometric average of their log-transformed expression values to guide normalization (geNorm method).

Methods of the third class, which are *based on genes selected from the data* (Fig. 2, bottom), start by identifying a (usually large) set of genes expressed in the samples to be compared, and then use various combinations of these genes to derive the scaling factors that render the samples comparable. The TMM algorithm is one such fully data-driven method, based on pairwise sample comparison of "double trimmed" genes (i.e., trimmed first by absolute expression level ranks within each sample, and then by expression ratios between the two samples). We explored a variety of novel methods that use single trimming (by expression level ranks within each sample) and that scale all samples simultaneously. In particular, we created the novel Network Centrality Scaling (NCS) algorithm that uses pairwise gene co-expression as a similarity metric, and identifies the most central genes in the resulting network. These central genes are particularly suited to serve as normalization guides.

Finally, scaling methods can be devised *using randomly picked values* (Fig. 2, top). In particular, we implemented an Evolution Strategy algorithm that stochastically identifies

solutions that maximize, as objective function, the number of genes expressed uniformly across samples.

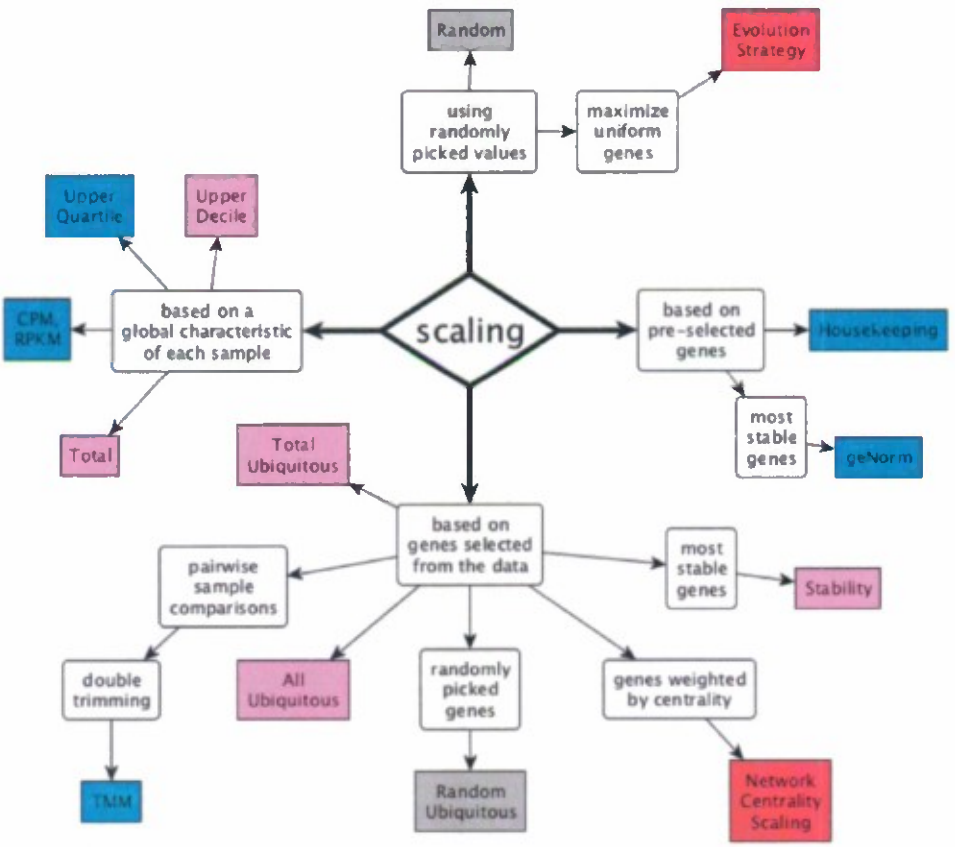

Figure 2. Taxonomy of normalization methods.

Even when based on very different concepts, the various normalization methods may share one or more computational procedures in common. We dissected the methods into distinct computational steps and identified shared components among the various algorithms. We organized these into a chart resembling a map of bus lines (Figure 3), leading from the raw data matrix (green "station" in Fig. 3) to one of three possible endpoints (red "stations"). In this visualization, "stations" represent intermediary results, and the lines connecting them represent computational steps. As shown in the figure, there are four different initial actions: 1) ignore the data except for the pre-determined housekeeping genes; 2) ignore the data entirely and select random scaling values; 3) use the data solely to compute the total expression in each sample; 4) sort the data matrix in preparation for a variety of more complex computations.

The sorted data matrix can then be used to compute rank-specific averages (for the Quantile Normalization method), to identify the expression levels at different percentiles of the distribution (for the upper quartile and upper decile methods), or to identify ubiquitous genes. Ubiquitous genes are then used by several methods in diverse ways.

Except for the CPM and Quantile Normalization methods, all the algorithms we describe here converge on a set of relative scaling factors, which we adjust to keep the global scale of the data set. These scaling factors can be computed from: 1) equal gene weights, 2) variable gene weights, 3) whole-sample weighted means, 4) a target value per sample, or 5) random values.

We found that best results are obtained with methods involving stochastic optimization, and with certain methods based on analysis of ubiquitous genes.

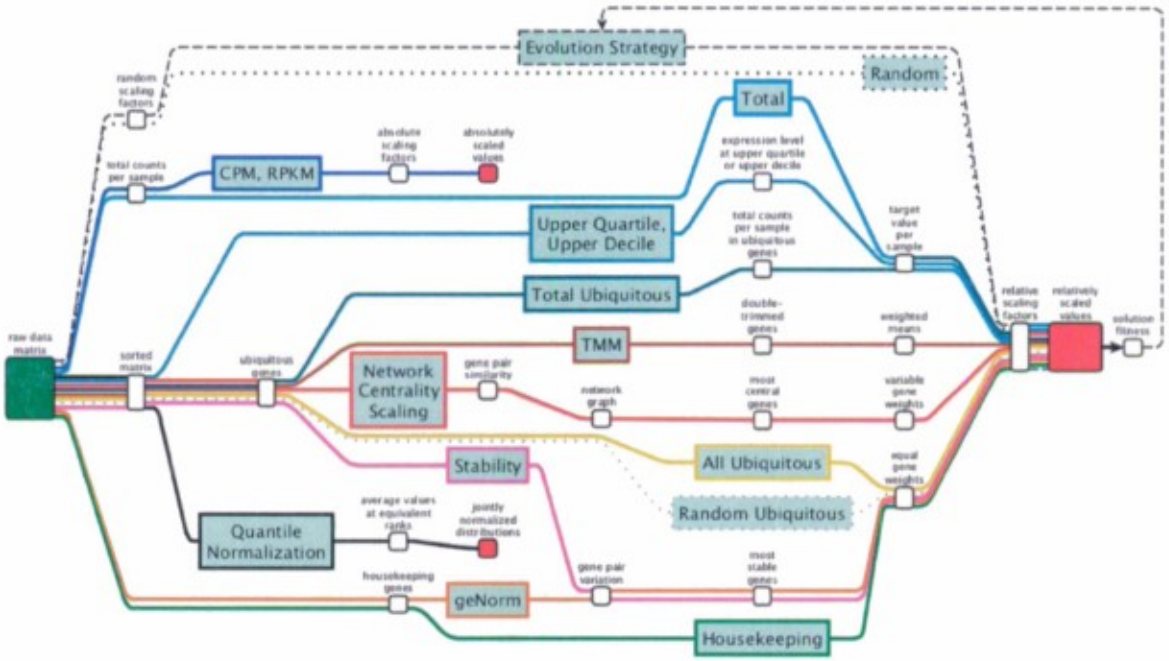

Figure 3. Computational pathways for normalization.

Qualification of success of normalization methods: The availability of many normalization methods, which produce different results, poses the more complex question of how to assess which result is correct. We devised three different ways of evaluating the diversity of solutions from the different algorithms.

1) Maximization of uniform genes. We defined uniform genes as those with very similar expression levels across all samples studied. Mathematically, we used a stringent upper cutoff on the coefficient of variation. Successful normalization methods adjust expression values in such a way that a larger number of genes reach uniformity. Importantly, this metric (number of uniform genes) can be used as an objective function, which can be optimized using stochastic algorithms. We implemented an Evolution Strategy (ES) to do this. The ES consistently identifies the best solutions based on this criterion (Figure 4).
2) Maximal decorrelation of sample rankings. We found that, under improper normalization, different genes tend to rank samples (by expression levels) similarly. Conversely, more successful normalization methods minimize this correlation (Figure 5). We further found that our best methods bring the average correlation to nearly its theoretical absolute minimal value - zero. This suggests that the methods are not just successful - they approach optimality.

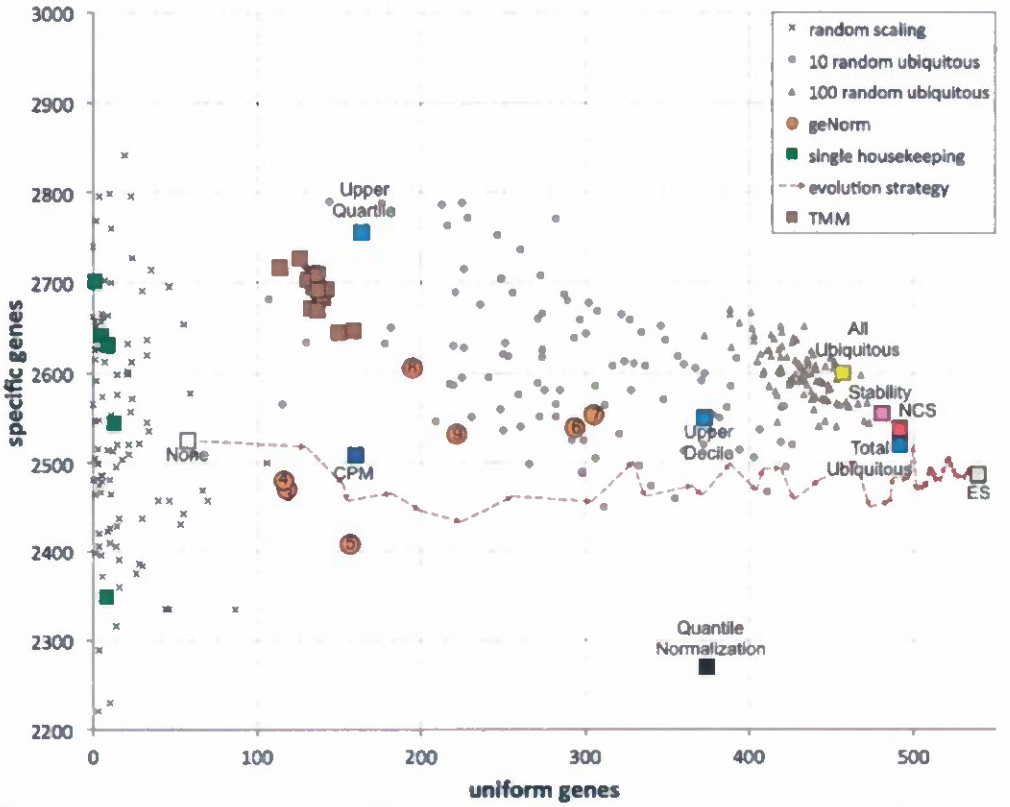

Figure 4. Number of genes identified as specific to one sample vs. number of genes observed to be consistently expressed across samples, for various normalization methods. The numbers in the orange circles denote the number of housekeeping genes combined using the geNorm algorithm. The dashed arrows show the stochastic path of the ES from the data prior to normalization (white square, "None") to the best approximation to the optimal solution (gray square, ES). Brown squares represent the results obtained via the TMM method, using each of the 16 samples as reference.

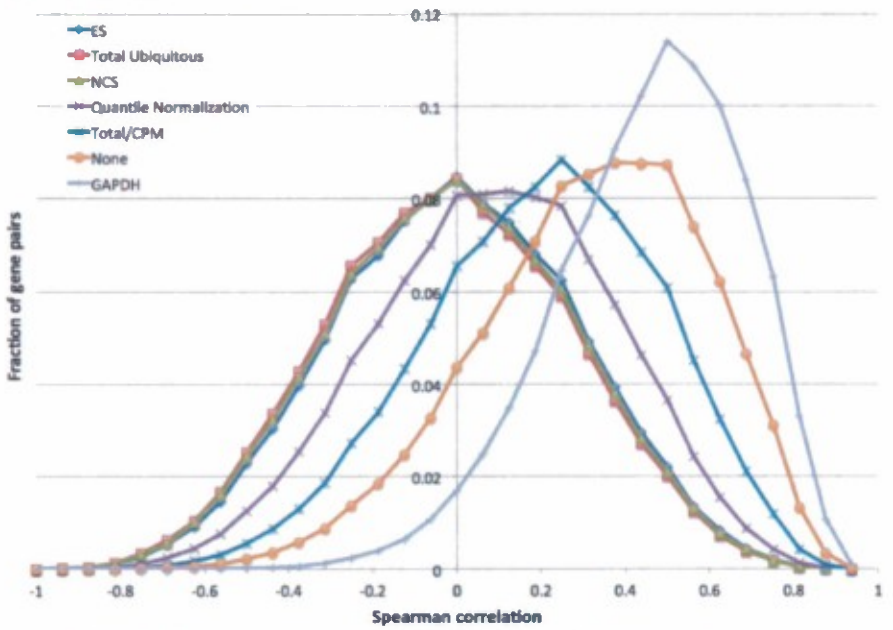

Figure 5. Density distribution of Spearman correlations of sample rankings for some normalization methods.

3) Similarity among solutions. While many methods produce very different solutions to the normalization problem, a subset of them produce similar results (Figure 6). These methods are conceptually and computationally very different from each other, and yet they converge on a common solution. This is also the solution that maximizes uniform genes and maximally decorrelates samples, lending it strong credence.

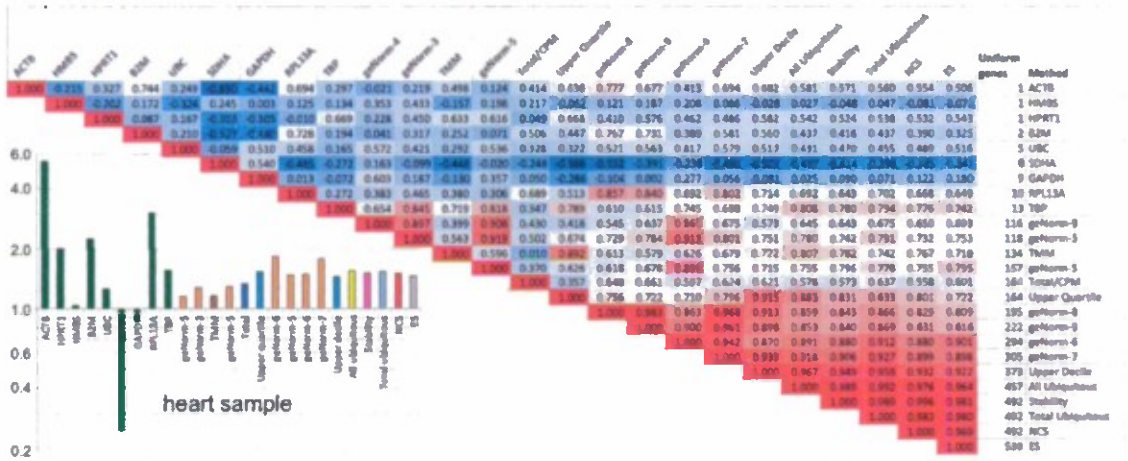

Figure 6. Comparison between the scaling factors suggested by the different methods. Lower left: the resulting scaling factors for the heart sample. Upper right: Pairwise correlations between the methods, for all samples. Red shades denote high correlation values (above 0.75), blue denotes low correlation (or anticorrelation). The column to the right indicates the number of uniform genes identified by the method. The Quantile Normalization method is not included in this analysis since it does not produce scaling factors.

Analysis of tissue specificity: We analyzed the resulting gene expression values following normalization with various protocols. We used a few definitions to identify uniform, specific, enriched and depleted genes:

1) Background noise level. We considered genes with a median expression value under 10 reads to be at noise level.

2) Variation bandwidth. We considered a two-fold change in expression (up or down from the median) to be within "acceptable limits", beyond which a gene may be differentially expressed.

3) For the purpose of this analysis, we considered genes as "uniform" if their median level is above background, and all samples were within the variation bandwidth around the mean.

4) We considered a gene to be "specific" to a sample (or to two) if its median expression is within noise level, but above the variation bandwidth for the single sample (or both samples).

5) We similarly considered a gene to be "enriched" to a sample (or to two) if its median expression is above noise level, and above the variation bandwidth for the single sample (or both samples).

6) We considered a gene to be "depleted" in a sample if its median expression is above noise level, but below the variation bandwidth for the single sample (or both samples).

In this example comparison (Table 1) between raw data (no normalization), normalization to total counts, and the network centrality scaling as an approximation to the optimal scaling solution, we see that successful scaling yields much larger numbers of uniform genes, as expected.

Genes	Raw	Total/CPM	NCS
Uniform	513	1002	1559
Specific (to 1)	3790	3723	3648
Specific (to 2)	2139	2224	2185
Enriched (in 1)	474	842	1323
Enriched (in 2)	256	418	628
Depleted (in 1)	848	1020	824
Depleted (in 2)	661	521	349

Table 1. Uniform, specific, enriched and depleted genes for the raw data, or after normalization to 'total' counts (equivalent to counts per million) or Network Centrality Scaling.

If a gene is not observed (or observed at noise levels) in any sample except for one, it will be trivially identified as specific to that sample. Such determination is largely unaffected by normalization, and indeed the number of "specific" genes changes little. When the expression level in the specific sample is low, there is room for a false-positive determination of specificity. Proper normalization may correct this, yielding somewhat fewer specific genes, as observed.

When the expression level in most samples is significantly above noise level but one sample (or a few) have significantly higher expression levels, the gene is also specifically expressed in that sample. We call this "enriched" in that sample, for simplicity. Identifying "enriched" genes is not trivial, and strongly susceptible to normalization. The number of tissue-enriched genes identified by the optimal scaling methods is much larger than by simpler (e.g., CPM) methods or in the raw data. This is a beneficial result that was not imposed by the normalization methods themselves, and we count this as additional evidence for successful normalization.

We explored also the symmetric situation, in which just one sample shows a significantly lower level than the rest ("depleted" genes). This situation can reflect a true biological effect, though infrequently so. It is much more common to observe this situation as a result of improper normalization, e.g., when normalizing by CPM, a highly expressed tissue-specific gene may cause other gene expression values to be downgraded, resulting in their apparent "depletion".

Publications: The work described above is being prepared for publication. "Optimal Scaling of Digital Transcriptomes" Gustavo Glusman, Max Robinson, Burak Kutlu, Juan Caballero and Leroy Hood. An earlier version of this manuscript has received DOD approval.

Software: The software for these analyses is under continuous development, and can be found here: http://db.systemsbiology.net/gestalt/normalizer/

Biomarker studies on the mouse model system

Aim 2: Analyze the bloods and multiple organs/tissues of animals from three inbred mouse strains exposed to the toxins acetaminophen and carbon tetrachloride for transcriptomes, proteins and miRNA biomarkers.

Aim 3: Establish MRM mass spectrometry assays for at least 25 liver-specific blood proteins based on the acetaminophen, CCL4, and other model systems of interest.

Aim 4: Analyze the bloods and tissues of animals from three inbred mouse strains exposed to the toxins acetaminophen and carbon tetrachloride for protein biomarkers

using proteomics technologies, including MRM.

Because these three aims are all interconnected, we report progress for all of them together, first describing work done in proteomics, and then work done on transcriptomes.

Several ISB researchers worked on these aims, with the result that multiple proteins identified as being likely to be primarily liver-specific biomarkers were identified in the blood using various mass spec and antibody-oriented technologies. Two sets of *in vivo* mouse experiments were done using acetaminophen perturbation. In one of these sets (described in A, B and D below), time course measurements were analyzed on each animal separately, revealing the wide range among individual animals in terms of their response, even though we used an inbred strain (results are. In the other set (described below in C), which was done first to get a lay of the land, animal samples collected at various time points were pooled.

The first report on these three aims is from Shizhen Qin, who describes the experimental methods and results, with a focus on using MRM mass spectrometry to identify biomarkers indicative of acetaminophen and CCL4 exposure damage. The second report is from Bingyun Sun, who has examined protein abundance changes in several organs after exposure to acetaminophen. The third report comes from Chris Lausted, Zhiyuan Hu, and Hyuntae Yoo who did the initial biomarker survey experiments with pooled mouse samples. Finally, Kai Wang reports his work analyzing the effects of acetaminophen treatment on the mouse liver transcriptome.

A. Mouse model system and MRM results (Shizhen Qin reporting).

Introduction: In the assessment of liver damage by drugs and chemicals, the determination of enzyme levels such as ALT (alanine transaminase) and AST (aspartate transaminase) is largely used. Necrosis or membrane damage releases the enzymes into circulation; therefore, they can be measured in blood. AST (AST1 and AST2) are mainly distributed in heart, muscle, brain, liver and kidney. Any damage of these tissues will result in releasing of AST protein into blood stream and is therefore not highly liver specific. For example, following a myocardial infarction, serum levels of AST are elevated and reach a peak 48 to 60 hours after onset. ALT1 is about 3-4 fold more enriched in liver followed by kidney, heart, muscle pancreas and lung and is more liver specific than AST. However, ALT2 is similar to AST that is, not enriched in liver more than in many other tissues and is mainly found in muscle, liver, heart, pancreas, prostate and spinal cord. In laboratory blood tests employing colorimetric and ultraviolet catalytic enzymatic reactions for the quantitation of ALT and AST, both ALT and ALT isoenzymes 1 and 2 are detected due to lack of ability to measure each isoenzyme activity separately. In addition to problems with liver specificity, half-lifes of both enzymes in the blood stream are short, ALT and AST activities only present in blood for a short period of time after liver injuries occurred. New, better liver injury markers are needed. In this project, we employed known liver toxins acetaminophen (APAP) and carbon tetrachloride (CCl4) in mouse models with liver-specific proteins as targets and mass spectrometry technology SRM (selected reaction monitoring) for quantitative proteomics to discover new potential markers for liver injuries induced by these two types of chemicals.

Brief description of materials and methods:

1. Animals, drug treatment and plasma preparation

In the pilot studies, we tried three inbred mouse strains: C57BL/6J, A/J and SJL from the Jackson Laboratory and found that all three strains responded to APAP and CCl4 liver toxicities similarly as measured by the elevations of blood ALT and AST levels. The fourth mouse strain tested, NOD/ShiLtJ, proved more sensitive than the three mouse strains tested to both APAP and CCl4 toxicity as judged by earlier responsive time and higher ALT and AST levels in the blood after treatment. Therefore, C57BL/6J (B6) and NOD/ShiLtJ (NOD) were used for the full tests. (Mouse blood and tissue samples were used for the analyses described below)

Female B6 and NOD mice 8 weeks of age were injected intraperitoneally (IP) with 375 mg/kg of acetaminophen dissolved with PBS or 1ml/kg CCl4 diluted 1:10 with sterile Corn oil. Control animals received the same volume of PBS (acetaminophen controls) or corn oil (CCl4 controls) at each time points. Blood was drawn at 3, 8, 12, 24, 48, 72, 96 hours after injection for SRM analyses. For western blot analyses, time points were extended to 120, 144 and 168 hours. Mice receiving APAP or PBS were fasted for 24 hours before injection (fasting started from 9:30am). No fasting was done for CCl4 treated and corn oil controls. The number of mice treated at each time point is summarized in Table 2.

	No treatment	3h	8h	24h	48h	72h	96h	120h	144h	168h
APAP/B6	3	5	5	10	9*	3	3	6*	6*	5*
PBS/B6		3	3	3	3	3	3	2	2	2
APAP/NOD	3	5	10	5	5	7	5	8	8	5*
PBS/NOD		3	3	3	3	3	3	2	2	2
CCl4/B6	3	3	3	2*	3	3	3	4	4	4
Corn oil/B6		3	3	3	3	3	3	2	2	2
CCl4/NOD	3	3	3	3	3	3	3	4	4	4
Corn oil/NOD		3	3	3	3	3	3	2	2	2

Table 2. Number of mice treated at each time point. Controls were treated with PBS (for APAP) and corn oil (for CCl4). Due to drug treatment related death, mouse number labeled with * indicates number of survivals at that time point.

Blood samples were drawn by Cardiac Puncture. Typically, 400ul blood was obtained from each mouse. Plasma was prepared flowing Tammen's method (see references at end of this section). Plasma samples were stored at -80°C without proteinase inhibitors.

All work for this project involving live animals was conducted under Institutional Animal Care and Use Committee (IACUC) approved protocols (10-00 series). ISB has an Assurance on file with the Office of Laboratory Animal Welfare (OLAW Assurance #A4355-01) and is accredited by the Association for Assessment and Accreditation of Laboratory Animal Care (AAALAC Accreditation #001363). All animal works were performed in our Pathogen Free (SPF) vivarium facility.

2. Quantitate AST, ALT levels in treated and control mouse plasma

Plasma ALT and AST levels were determined colorimetricly by using ALT, AST reagent kits following the manufacturer's instructions (TECO Diagnostics, Anaheim, CA). Specimens were analyzed on the day of collection. Duplicated measurements were performed.

3. Blood Acetaminophen concentration measurement after injection

Blood acetaminophen concentrations were measured in plasma with an acetaminophen

Elisa kit with less than 2% cross reactivity of other compounds such as procainamide (Neogen Corporation, Lexington, KY). All tests were performed following the instruction manual provided.

4. Plasma sample preparation for SRM

To reduce the complexity of proteins in the plasma samples, the top 14 highly abundant proteins were depleted. Depleted plasma were digested with trypsin and desalted with Oasis MCX cartridges (Waters, Milford, MA).

5. Preparation of the liver-specific and liver-enriched proteins list

We used a targeted approach focusing on organ-specific proteins to increase the likelihood of identifying protein biomarkers in blood that may reflect pathology of a particular organ. Our list of liver-specific or liver-enriched proteins (liver proteins) was created by analyzing tissue-specificity in RNA datasets and by performing an organ-specific protein search with Gene Atlas Interface analysis. The mouse databases searched against were 3 datasets from NCBI-GEO (Gene Expression Omnibus) with a total of 179 mouse tissues. Due to the similarities of mice and human genome, human proteins that were identified by us (Qin et al, 2012 in preparation) as liver-specific or liver-enriched were also included in the mouse liver protein list.

6. Peptide selection from the liver protein list

The mouse liver protein list contains 165 proteins of which 131 were previously detected by mass spectrometry. A total of 547 peptides suitable for SRM analyses were selected from 116 of the 131 previously detected liver proteins. Two to three peptides were selected from each protein following peptide selection criteria for SRM (Lange, et al., 2008). Peptides previously identified in PeptideAtlas (Deutsch et al., 2008) were preferentially chosen.

All peptides used in this study were checked by BLAT at http://genome.ucsc.edu/ and Protein BLAST (http://blast.ncbi.nlm.nih.gov/Blast.cgi) searches to ensure that they are unique to the target protein at both proteomic and genomic levels. Finally, the uniqueness of every Q1/Q3 pair from the target peptides were confirmed by an SRM theoretical collision calculator tool (http://proteomicsresource.washington.edu/cgi-bin/srmcalc.cgi)

7. Monitoring liver-specific proteins in blood by SRM

All SRM analyses were performed on an Agilent 6460A triple quadrupole (QQQ) mass spectrometer with a ChipCube nanoelectrospray ionization source coupled with an Agilent 1200 nanoFlow HPLC system.

7.1 Detection of endogenous peptides in pooled plasma samples from control and treated animals

From 131 liver proteins that were previously detected by Mass Spec, 547 peptides were selected from 116 proteins that meet the peptide selection standards. We performed endogenous peptide (all-light peptide as opposed to heavy peptide standard) SRM analyses in an effort to find out how many of the native proteins and their peptides could be detected in control and treated mouse plasma samples before heavy peptide standards were purchased. From this all-light test, we have detected 199 peptides representing 81 proteins. Crude unpurified peptide standards (heavy peptides) that correspond to the detected natural counterparts (light peptides) were synthesized with heavy isotopic lysine (13C615N2) or arginine (13C615N4) at the C-termini (Sigma-Aldrich, USA).

7.2 Collision energy optimization and heavy peptide titration
Collision energies (CE) determined using the default formula from Agilent were further optimized with 4 additional CE steps (±5V, ±10V). The best precursors and each of their 4 transitions under optimized conditions were selected (Figure 7). Detected heavy peptides were titrated at 6 concentrations in a normal human serum background to build a titration curve and to determine the proper amount of each peptide standard to spike-in (Figure 8).

7.3 Full SRM tests
Based on titration curves, a proper amount of heavy peptides were spiked in to each plasma samples to reach a L/H ratio within ± 10 fold in most cases. One to two mice (mouse #1 and 2) from each control group at all time points were analyzed by SRM. For CCl4 treated mice, two treated mice (mouse #1 and 2) were analyzed at each time point in both NOD and B6 strain. As for APAP treated mice, due to the great response variations to the treatment at different time points after treatment, 4 mice and 3 mice were analyzed at 8 hour and 24 hour time point, respectively for APAP/NOD and 4 mice and 5 mice were analyzed at 24 hour and 48 hour time point, respectively for APAP/B6. Duplicated runs were performed for each sample.

8. SRM data analysis
All SRM data were processed using the Skyline Targeted Proteomics Environment (v1.1) (MacLean et al., 2010). All data were manually inspected to ensure correct peak detection and accurate integration. Peptides with at least 3-fold signal-to-noise ratio were considered detectable. The total peak area and Light/Heavy ratio of each peptide were exported for statistical analysis.

9. Statistic analysis
All other analyses including calculation and graphics were generated by scripts written by computational biologists at ISB or by Prism 5 graphics software (GraphPad software, La Jolla, CA, USA).

10. Western blot analysis
To investigate the detectability of potential new marker proteins in plasma by Western blotting, plasma (not depleted) samples from treated and control mice were loaded on protein gels and proteins in each sample separated. The proteins were transferred to PVDF membrane and probed with primary antibodies, washed and incubated with HRP-conjugated secondary antibodies. Detections were carried out and the images were analyzed using ImageJ.

Results:

1. Mouse liver injuries induced by IP injection of APAP and CCl4 measured by ALT and AST values
Responses to the treatment of drugs in mice were judged by the increase of ALT and AST enzyme activity in the plasma. To CCl4 treated mice, Variations between individual animals in both B6 and NOD strains were small. However, we observed huge individual differences in terms of drug responsiveness to APAP injection in both mouse strains at the peak responsive time points. In all cases, we noticed AST elevations and ALT elevations paralleled each other and therefore only ALT values are cited throughout this

study. The ALT values after treatment in both strains by the two drugs were summarized in Figure 7.

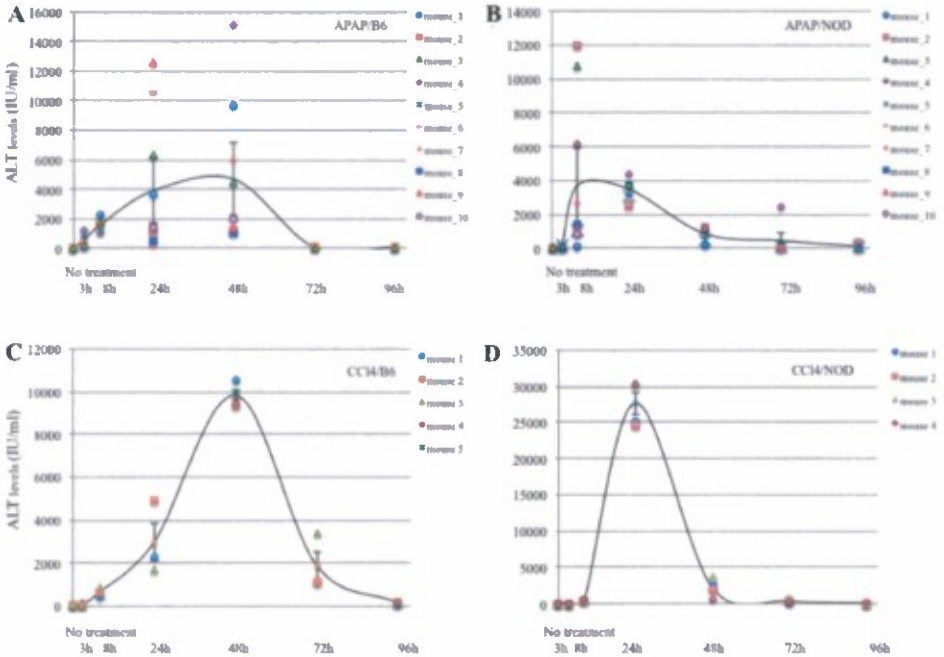

Figure 7. Huge variation among mice at the peak responsive time points indicated by plasma ALT levels were observed after APAP treatment in both B6 (A) and NOD (B) mice. Uniformed results were obtained after CCl4 treatment in both B6 (C) and NOD (D) strains. Black smooth curve lines: average ALT levels after treatment with STDEV error bars.

Blood APAP concentration tests performed in plasma at 3 and 8 hour time points after drug administration in both NOD and B6 mice shown consistent acetaminophen concentrations in blood of highly responsive, low responsive and non-responsive animals. This fact indicates that the inter-individual differences among animals to APAP treatment is not due to incorrect introduction of the drug into the animal systems (Table 3).

Sample name*	APAP plasma concentration (μg/ml) at 3 hour after injection**	ALT level (IU/ml)
NOD/3h_1	98	53
NOD/3h_2	91	126
NOD/3h_3	111	66
NOD/3h_4	107	95
NOD/3h_5	89	212
B6/3h_1	51	102
B6/3h_2	52	280
B6/3h_3	40	264
B6/3h_4	33	1242
B6/3h_5	39	910

Table 3. No association of plasma APAP concentration to liver toxicity indicated by ALT levels 3 hours after injection in both mouse strains. *Sample name: Strain/time point_mouse number. ** At 8 hours after injection, all mouse plasma APAP concentrations fall to zero in both strains.

2. Identification of liver proteins

Using strategies described above, by mining the gene expression data, we identified 165 mouse liver proteins. All these proteins' human counterparts have passed GeneCards (a human only database) verification.

3. Endogenous proteins detected by SRM and confirmed by heavy peptide standards

After suitable peptides and transitions for each liver protein were selected, we used pooled control and treated mouse plasma to determine how many liver proteins can be detected by SRM. Eventually, we have detected 142 peptides derived from 81 liver proteins by SRM and all of them were confirmed by synthetic corresponding heavy peptides spiked-in.

4. CE optimization

Collision energy optimization was performed as described in Methods. Duplicated runs were performed for each CE. A total of 284 charge 2 and charge 3 precursors from 142 peptides were optimized. Best transitions and collision energies were used for SRM full tests.

5. Consistency and accuracy of SRM data

5.1 Duplicate SRM runs are well correlated

Duplicate runs were performed for each sample; technical variations between the two runs were small as exemplified with two runs of peptide FVEGLPINDFSR in the CCl4/NOD study (Fig 8A). In general, Pearson tests showed good correlations between runs (> 0.9 in most cases).

5.2 Protein levels measured by multiple features are consistent

When a protein level is measured by more than one peptide, close agreement in quantification was observed. This observation gave us reasonable confidence that protein levels in samples estimated from a single peptide from a given protein can be reliable (Figure 8B).

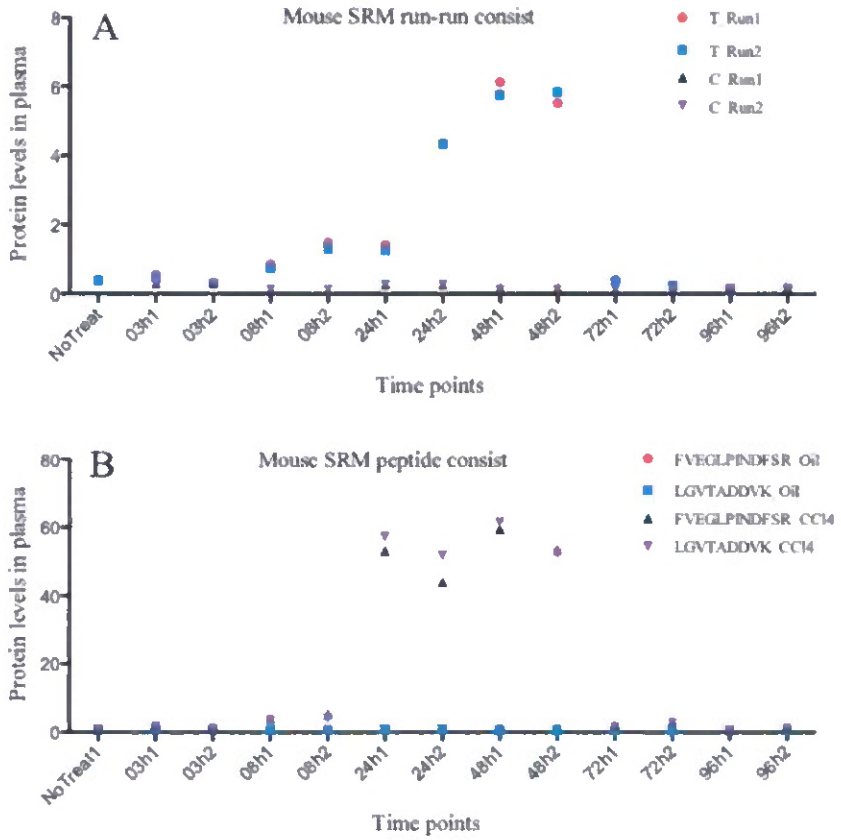

Figure 8A. MRM analysis. Variations between technical replicates were generally small with a Pearson correlation value >0.9 between duplicate runs, plasma protein levels of measured by peptide FVEGLPINDFSR in the CCl4/NOD test were consistent. T run_1, treated first run; T run_2, treated second run; C run_1 control first run; C run_2, control second run. 8B. Multiple peptides derived from the same protein performed consistently in most SRM tests. As shown here, protein plasma levels measured by two different peptides selected from the same protein were in close agreement. Relative protein levels in plasma are indicated by normalized light/heavy peptide ratios.

6. Thirty informative proteins were found to distinguish controls and APAP or CCl4 treated mice

From the 81 proteins tested by SRM in this study, we identified 30 proteins (known liver markers AST1 and 2 included) that are able to separate drug treated mice from their controls. These 30 proteins fall into 4 categories: 1) As good: protein levels higher in treated animals that are basically as significant as ALT and AST levels measured with the colorimetric enzymatic reactions and by SRM (AST1 and AST2); 2) Worse: proteins levels are higher in treated animals but the differences are less significant than detected by ALT and AST; 3) Potentially better: protein levels higher in treated animals that are potentially better than ALT and AST as liver injury markers; and 4) Leverl down: protein levels that are lower in treated mice than in controls. The results are summarized in table 4.

Non-informative	Informative			
	Potentially better	As good	Worse	Level down
51 (63%)	8 (10%)	13 (16%)	5 (6%)	4 (5%)
Protein 1	Protein 4	Protein 2	Protein 5	Protein 54
Protein 3	Protein 6	Protein 17	Protein 31	Protein 67
Protein 7	Protein 15	Protein 18	Protein 38	Protein 75
Protein 8	Protein 16	Protein 33	Protein 53	Protein 81
Protein 9	Protein 19	Protein 37	Protein 56	
Protein 10	Protein 24	Protein 46		
Protein 11	Protein 45	Protein 48		
Protein 12	Protein 50	Protein 52		
Protein 13		Protein 62		
Protein 14		Protein 64		
Protein 20		Protein 71		
Protein 21		Protein 79		
Protein 22		Protein 80		
Protein 23				
Protein 25				
Protein 26				
Protein 27				
Protein 28				
Protein 29				
Protein 30				
Protein 32				
Protein 34				
Protein 35				
Protein 36				
Protein 39				
Protein 40				
Protein 41				
Protein 42				
Protein 43				
Protein 44				
Protein 47				
Protein 49				
Protein 51				
Protein 55				

Protein 57				
Protein 58				
Protein 59				
Protein 60				
Protein 61				
Protein 63				
Protein 65				
Protein 66				
Protein 68				
Protein 69				
Protein 70				
Protein 72				
Protein 73				
Protein 74				
Protein 76				
Protein 77				
Protein 78				

Table 4. Results of SRM analyses of the 81 liver proteins searched for liver injury markers. Existing liver marker AST (AST1 and 2) are included as informative proteins in the "as good" category. Protein names are denoted as Protein 1 to Protein 81 before publication (protein names will be provided upon request by DOD). "Better", "as good" and "worst" are terms to describe the new markers as compared to the classic liver markers ALT and AST. "level down" markers have lower plasma protein concentrations in treated animals than in controls.

6.1 Eight proteins are shown potentially better as liver injury markers in our animal models than the existing liver marker ALT and AST

The power of the strategy of using liver specific proteins as targets combined with SRM technology was demonstrated in this study by revealing 30 proteins that are informative to liver injuries caused by chemical exposures. More significantly, we have found 8 proteins that performed better in at least one drug/strain combination in this study and may potentially serve as better markers than ALT and AST for liver injuries.

6.2 Five proteins are confirmed significantly better than ALT and AST

Out of these 8 proteins, we are particularly interested in five: Protein 45, Protein 19, Protein 6, Protein 4 and Protein 16. Protein 45 is interesting because its extended presence in plasma widened the detectable period of liver injuries caused by CCl4 in NOD mice from a narrow window (sharp peak at 24 hours after treatment) to 24-168 hour after drug injection. This elongated damage-detectable period is also true in the other mouse strain/drug combination after CCl4 treatment.

Alternatively, Protein 19 levels in plasma start to show increase at 3 hours and reach peak value 8 hours after treatment and this protein acts as a better marker for early detection of CCl4 caused injuries. A combination of Protein 19 and Protein 45 will cover the detectable period of CCl4 induced liver injuries in NOD mice from 3 hours to at least 168 hours after drug treatment. Similar results were obtained for CCl4 induced injuries in B6 mice except that the peak responsive time point to the toxic effect of CCl4 was at 48 hour after treatment. On the contrary, ALT and AST are indicative mainly at 24 hours for

NOD mice after treatment. The results of Protein 19 and Protein 45 as markers for CCl4 induced liver injuries in NOD mice are summarized in Figure 9.

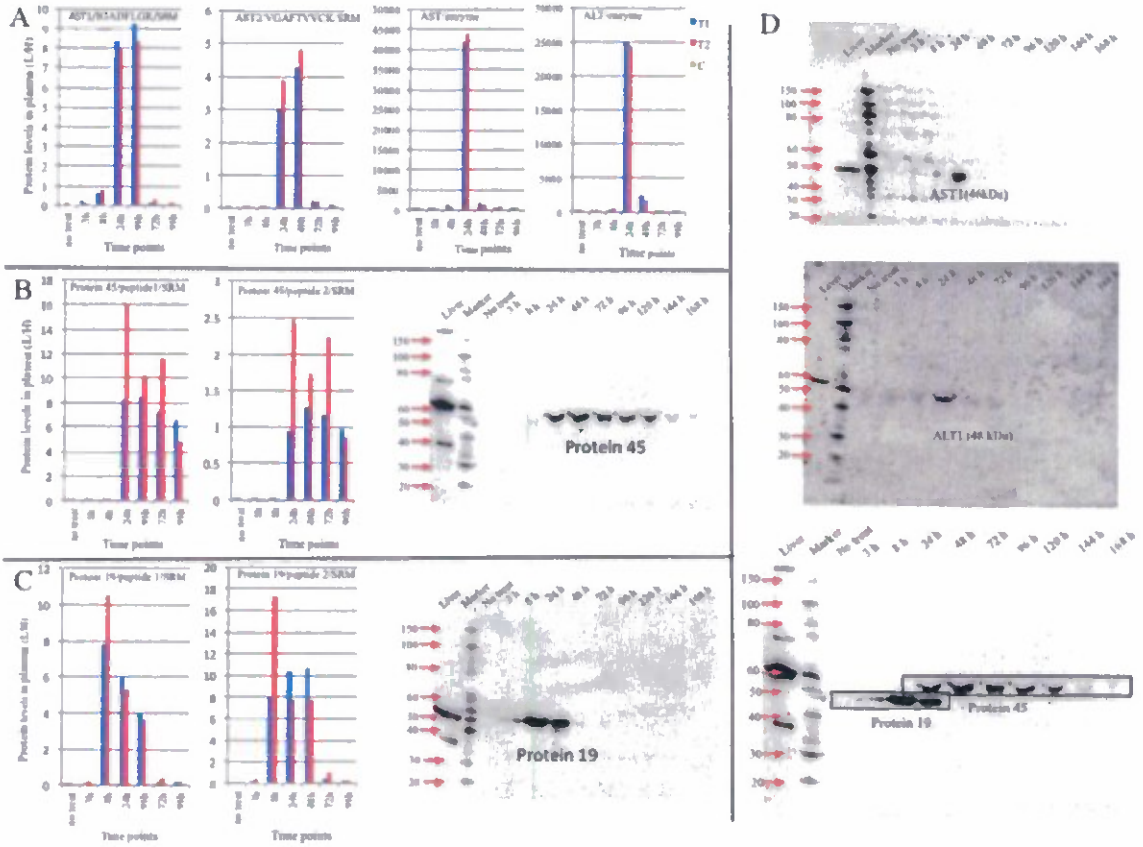

Figure 9. Combination of protein 19 and Protein 45 are superior to ALT and AST in detecting liver injuries induced by CCl4 in NOD mice. A) SRM and enzymatic reaction data at time points after exposure to CCl4. AST1 and AST2 levels in plasma elevated mainly at 24 and 48h time points as measured by SRM and at 24h time points by enzymatic reactions. B) Protein 45 levels are significantly higher from 24 to 96h (measured by two Protein 45 peptides in SRM analysis) and Western blot analysis is consistent with SRM results. By using Protein 45 as liver injury marker, the detectable period is extended to at least 168 hours after treatment. C) Protein 19 levels were detected early at 3h after treatment with CCl4 and were still highly detectable at 48h time point (measured by SRM with two Protein 19 peptides and by Western blot). D) top: Western blot image of AST1. AST1 protein band shown mainly at 24h time point after treatment. Middle: Western blot image of ALT protein. Bottom: Western blot image shown a combination of Protein 19 and Protein 45 successfully detected liver injuries from 3 to 168 hours after CCl4 exposure. Similar results observed in B6 mice treated with CCl4. T1: treated mouse 1; T2: treated mouse 2; C: control mouse 1 at each time point. In all cases, mouse 1 at each time point was used for Western blotting.

In acetaminophen-treated NOD mice, the peak responsive time point is at 8 hours after treatment. At the 3-hour time point, test results of both mouse 3h1 (3-hour time point mouse number 1, and so on) and 3h2 ALT enzyme failed to show any level increase although pathologic microvesicular changes are clearly shown. However, Protein 4 levels measured by SRM demonstrated significant increase at the 3 hour time point. Similarly, at the 96 hour time point, mice 96h4 showed no increase of ALT level. However, the increases of Protein 45 levels for corresponding mice were significant. More impressively, western blot results of AST1, AST2 and ALT only revealed a protein

band at the 24 hour time point for ALT, 8 and 24 hour time points for AST1, and 24, 72 hour time points for AST2. Alternatively, Western blot results also demonstrated that Protein 45 is a better marker than ALT and AST at the corresponding 24, 48, 72, 96 time points with clear Protein 45 bands shown in each lane. The results of enzymatic reaction of ALT, SRM results for Protein 4, Protein 6, Protein 16, and Protein 45 in APAP treated NOD mice with corresponding Western blot gel results are summarized in Table 5.

Time points	No treat	3h 2	8h 2	24 h4	48h 2	72h 4	96 h4	120 h2	144 h2	168 h2
Protein/peptide	Enzyme/SRM/fold changes*									
ALT enzyme	1	1	118	43	12	24	1	1	1	1
Protein 4**	1	4	71	4	3	1	1	NT	NT	NT
Protein 6	1	1	66	43	51	121	1	NT	NT	NT
Protein 45**	1	1	10	239	557	1150	4	NT	NT	NT
Protein 16**	1	1	266	29	148	185	1	NT	NT	NT
Proteins	Western blot bands***									
GPT			▯							
AST1			▯	±						
AST2				±		±				
Protein 4	NT	NT	NT	NT	NT	NT	NT	NT	NT	NT
Protein 6		±	▯	▯	▯	▯				
Protein 45				▯	▯	▯	▯	▯	±	±
Protein 16		±	±	▯	▯	±	▯			

Table 5. Protein level changes listed in table 3 are from mice that are highly responsive to drug treatment at each time point. ALT protein levels in plasma were measured by enzymatic reactions (IU/L), Protein 4, Protein 6, Protein 16 and Protein 45 levels were measured by SRM (L/H ratios). Protein level fold changes were calculated by treated level/control level at each time point. NT: not tested.

* Less than >2 fold change of protein level is considered as fold of change = 1

** Protein in controls not detected. Used highest noise as control value to calculate fold of changes. Fold changes are relative. Fold changes in these cases are actually infinite.

*** ±, weak band; ▯, strong band; blank, no band. Protein 4 was not tested by Western blotting due to luck of good antibody.

Summary and discussion: We adopted a liver-specific protein based strategy for finding liver injury biomarker discovery in blood. The approach is centered on the idea that concentration of organ-specific proteins in the blood can be used to monitor the status of a specific organ because changes in blood concentrations reflect the normal as opposed to toxin-exposed and disease-perturbed status of their cognate biological networks. We mined transcriptomic databases to identify organ-specific proteins and created a 165 liver protein list. We used a mass spectrometry based SRM technology to selectively target liver-specific proteins in the blood from control and drug treated animals. We have established a workflow as illustrated in Figure 10. By using this SRM targeting liver protein strategy, we have assayed 81 liver-specific blood proteins based on the acetaminophen, CCL4 model systems in two mouse strains.

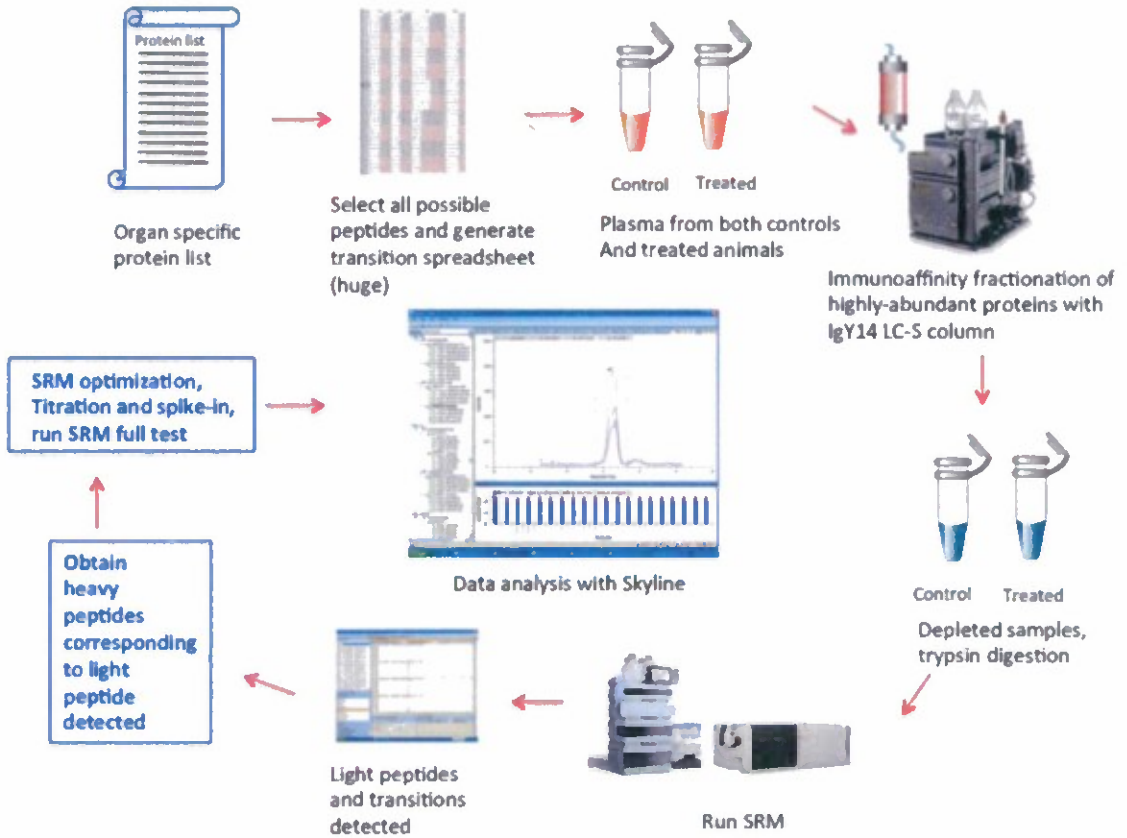

Figure 10. Workflow employed in this project for finding new liver injury biomarkers.

One of the greatest challenges in analyzing the plasma proteome is the complexity and extremely wide dynamic range of concentration of different proteins in the blood. Blood chemistry is the ultimate window into one's health. The human plasma proteome holds the promise of a revolution in disease diagnosis and therapeutic monitoring. Sampling blood is one of the least invasive methods of biological sample collection. However, blood contains tens of thousands of different proteins from all tissues plus numerous distinct immunoglobulin sequences with an extraordinary concentration dynamic range in 12 orders of magnitude. The extreme complexity and dynamic range of blood proteins made detection of individual protein of interest very difficult. To address this challenge, we adopted SRM technology to selectively monitor the limited number of proteins of interest (81 liver proteins) instead of randomly sampling a small portion of all blood proteins as by the mass spectrometry shotgun method. SRM can target specific peptides and proteins like antibodies without spending time and money to develop them, can be highly sensitive and can be high throughput and can be multiplexed to monitor >50 proteins in a single run. When used in combination with isotopically labeled standards it can also quantify levels of corresponding endogenous proteins in biologic samples. To effectively reduce the complexity of blood proteins, we used immunoaffinity columns to remove the most abundant proteins from the samples to allow for study of our less-abundant liver protein targets. The 14 most abundant proteins compose 90% of the total blood protein. Removal of the abundant protein resulted in a 10-fold enrichment of proteins of interest in the samples and an increase detection sensitivity. We observed significant sample-to-sample variations with the Seppro® IgY14 spin column in a separate study. The adoption of AKTA FPLC system coupled with a Seppro® IgY14 LC5 depletion column greatly improved the reproducibility of sample preparation (Qin et al,

2012). The sensitivity of the tests was further increased by careful optimization of collision energy and selection of the best-fit peptides and transitions. One of the key steps in our workflow that may have contributed to the success of finding new markers for liver injuries is that we performed pilot studies to investigate how many endogenous proteins can be detected under our SRM conditions not only in control plasma samples, but also in treated samples. If only the controls were used to reveal the detectability of liver proteins in plasma by SRM and monitoring these proteins for drug treated full tests, many targets would be missed because most of the promising new markers were present only in the circulating blood stream after drug induced liver damage accrued but not in untreated mice.

The power of this approach has been demonstrated from this study in which we have found 30 liver proteins that can be used to monitor liver injuries after chemical or drug exposure in mice. In addition, 5 proteins showed strong evidence that they might be potentially better than the long existing liver biomarkers ALT and AST.

Unlike AST and ALT enzymatic reactions, these 5 new protein markers can be integrated into antibody- or synthetic capture agent-based microfluidic chips (Integrated Blood-Barcode Chips), devices that have the potential to analyze large numbers of patient samples rapidly (in a few minutes), inexpensively, and in a highly multiplexed format (100s or even 1000s of different assays investigating many different diseases) employing blood from a pinprick.

Finding biomarkers has never been easy. Despite the fact that billions of dollars have been invested by big pharma, private investors and government grants, one new biomarker has been discovered each year on average. We have discovered and confirmed 5 proteins are superior to ALT and AST in mouse models. We believe that it would be a great waste if we stop here. We hope that we would have additional support to investigate these potential new liver markers in human subjects and explore the possibilities of conducting clinic trials with these new markers.

References: Manuscript in preparation: Qin, S., Gray, L., *et al.* Finding better blood markers for acute liver injuries induced by Acetaminophen and Carbon Tetrachloride. This manuscript has not yet been submitted to the DOD for approval.

Deutsch, E. W., Lam, H., Aebersold, R., PeptideAtlas: a resource for target selection for emerging targeted proteomics workflows. *EMBO Rep.* 2008, *9*, 429-434.

Lange, V., Picotti, P., Domon, B., Aebersold, R., Selected reaction monitoring for quantitative proteomics: a tutorial. *Mol Syst Biol.* 2008, *4*, 222.

MacLean, B., Tomazela, D. M., Shulman, N., Chambers, M., *et al.*, Skyline: an open source document editor for creating and analyzing targeted proteomics experiments. *Bioinformatics* 2010, *26*, 966-968.

Qin S, Zhou Y, Lok AS, Tsodikov A, Yan X, Gray L, Yuan M, Moritz RL, Galas D, Omenn GS and Hood L SRM targeted proteomics in search for biomarkers of HCV-induced progression of fibrosis to cirrhosis in HALT-C patients. Proteomics 2012, 12, 1–9

Tammen H. Specimen collection and handling: Standardization of blood sample collection.in Methods in Molecular Biology vol. 428: Clinical Proteomics: Methods and Protocols, Edited by A Vlahou. p35.

B. Analysis of multiple organ response to acetaminophen exposure (Bingyun Sun reporting)

Introduction: Blood is an ideal window for us to check disease and health status. Using mouse as an animal model for acetaminophen-induced toxicity study, I assessed acetaminophen-overdose multi-organ responses by analyzing the blood toxicoproteome. Tissue/organ specific protein signatures can leak or secrete into blood stream due to acetaminophen (APAP) toxicity. Clinical observation and animal studies have both indicated that acetaminophen idiosyncratic toxicity can impair multiple tissues and organs. To comprehensively examine such global responses, I developed a sensitive blood proteomics strategy as shown in Figure 11 that used immunodepletion to remove an abundant blood protein, albumin, a special N-terminal labeling technique for quantification purpose and a glycopeptide-capture method to fractionate blood proteome for non-glycopeptides and glycopeptides with glycans removed. All these efforts simplified blood protein complexity, and improved mass spectrometry (MS) identification and quantification accuracy. In the end, we successfully identified multiple organ responses of APAP in our mouse model, including kidney, heart, muscle, bone marrow, brain, intestine, and adipose tissues. Both Western blotting and targeted MS analyses were carried out and we successfully validated a list of organ specific proteins that can be used as location markers for disease, especially for toxicity diagnosis. Our results have agreed with previous knowledge about APAP toxicity collected through human and animal studies using techniques such as histopathology and radio-isotope tracing; and this is the first time to comprehensively discover multi-organ responses through a blood proteomics effort.

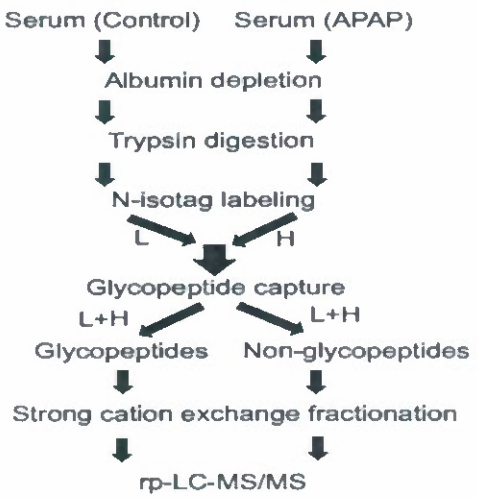

Figure 11. Illustration of the gagQP serum proteomics strategy, in which serum depleted albumin is subjected to denaturation and trypsin digestion, followed by labeling, glycopeptide-capture and reverse phase LC-MS/MS analysis.

Results: The major proteomics technical improvements for this study include first using a new N-isotag labeling reagent as shown in Figure 12 below. This new reagent increases MS identification efficiency of the labeled peptides; and the large mass shift between quantifiable biological samples created by this labeling reagent improves the flexibility of choosing the appropriate mass spectrometers for quantification. Secondly we adapted a glycopeptide capture method as a fractionation scheme here to simplify blood proteome

complexity and to remove glycan interference to MS identification of peptides as illustrated in Figure 11.

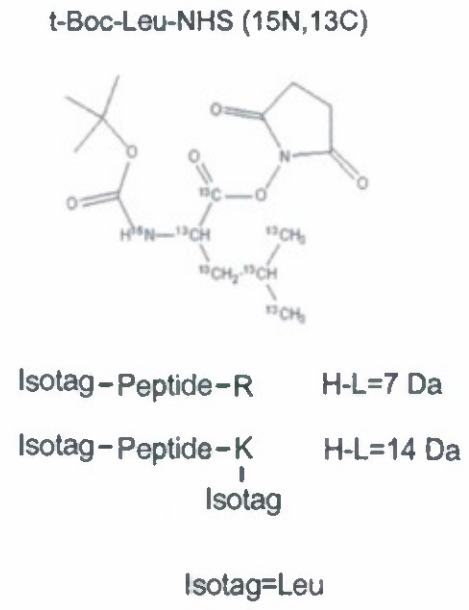

Figure 12. Chemical structure of the heavy formed (13C and 15N) N-isotag and its modification to peptides.

Using this strategy, we identified a list of organ-specific protein markers in blood and many of them showed responses to acetaminophen toxicity as summarized in Table 6.

Tissue	Gene symbol	MS quantification changes
Bone Marrow	Lcp1*	3.8
	Ltf	2.9
	Pip*	21
Brain	Ptgds	2.8
Fat	Me1	8.7
Heart/Muscle	Mb*	0.8
Muscle	Ckm	2.1
Kidney	Selenbp2(SBP)*	6.4
	Mdh1	6.4
	Sardh	8.S
	Umod	S.3
Skin	Car6	2.3
Intestine	Apoa4	2.1
	Fabp1	204
	Ppm1a	2.2

Table 6. Protein candidates identified for APAP overdose induced extra-hepatic responses derived from global MS survey, * highlights the proteins having been validated by Western as shown in Figure 13.

We validated both the organ specificity of the discovered protein markers as well as their responses in toxicity in blood. The Western blotting validation results are summarized in Figure 13. Our quantitative MS results also agreed well with observation made through other characterization approaches such as the use of surface plasma resonance array to measure protein concentration in blood as shown in Table 7.

A.

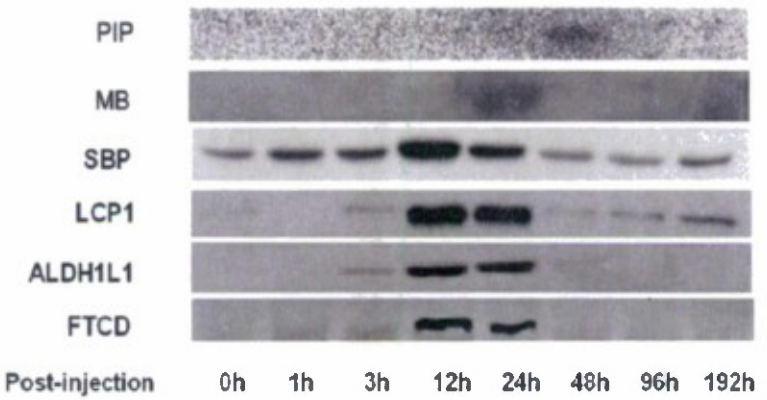

B.

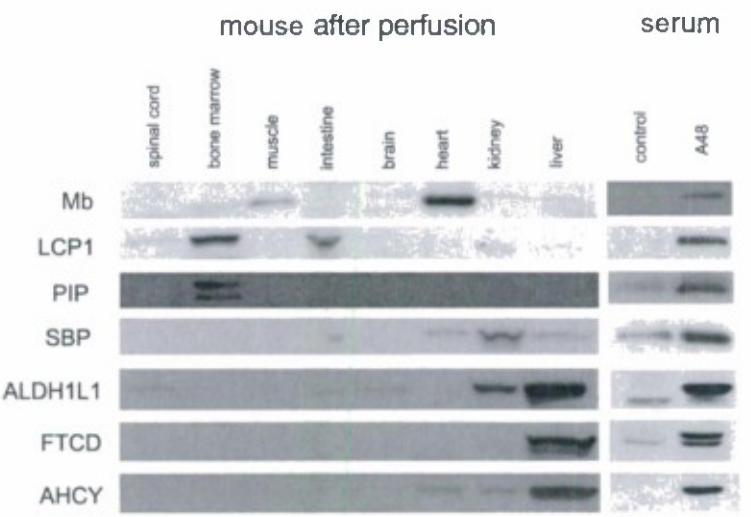

Figure 13. A: Western blot validation of mouse tissue specificity and response to drug in control and treated mouse sera of marker proteins identified through blood toxicoproteomics. B: Western validation of selected protein marker responses in mouse sera as a function of time after LD 50 APAP treatment.

#	Symbol	Toxicoproteomics	SPR
1	CPS1	▲	▲
2	ASL	▲	▲
3	CAT	▲	▲
4	GPT1 (SGPT)	▲	▲
5	GOT1(SGOT)	▲	▲
6	GLUD1	▲	▲
7	GNMT	▲	▲
8	FAH	▲	▲
9	MAT1A	▲	▲
10	Ahcy	▲	▲
11	Aldh1l1	▲	▲
12	ASS1	▲	▲
13	FBP1	▲	▲
14	Ftcd	▲	▲
15	ALDOB	▲	
16	HPD	▲	
17	BHMT	▲	
18	HGD	▲	

Table 7. Liver-specific proteins identified as differentially expressed in blood in response to APAP challenge by our toxicoproteomics and surface plasma resonance (SPR) techniques. Up and down solid triangle symbols indicate increased and decreased serum concentrations, respectively.

This proteomics effort for the first time to our knowledge demonstrates the strength of using high throughput MS protein analysis to comprehensively and sensitively identify global responses to drug toxicity. The organ specificity of the identified mouse protein markers has also been tested on human orthologous proteins. Many of these proteins carry the same tissue/organ signature property, thereby the validated organ marker proteins can be used directly to indicate the organ location of human diseases.

Publications: A manuscript is being prepared and will be submitted to DOD for approval.
Glycocapture-Assisted Global Quantitative Proteomics (gagQP) Reveals Multiorgan Response in Blood Toxicoproteome. Bingyun Sun, Jeffrey A. Ranish, Angelita G. Utleg, Zhiyuan Hu, Andrew Keller, Shizhen Qin, Cynthia Lorang, Li Gray, Amy Brightman, Denis Lee, Vinita M. Alexander, Robert L. Moritz, Leroy Hood

C. Summary of the pooled mice biomarker study (Christopher Lausted, Zhiyuan Hu, Hyuntae Yoo reporting).

Introduction: Over the course of this project, we utilized a mouse model and *in vitro* models to study liver injury, analyzed these biological models using novel antibody microarrays (see Aim 6 below) as well as immunoblotting and mass spectrometry, discovered fifteen new potential blood biomarkers, and developed novel antibody-based assays for these markers.

Biomarker Discovery: Using pooled mouse samples in a protocol following a time course after exposure to acetaminophen, fifteen liver-specific blood proteins were identified as markers of acetaminophen (APAP)-induced hepatotoxicity using three proteomic technologies: label-free antibody microarrays, quantitative immunoblotting, and targeted iTRAQ mass spectrometry. Liver-specific blood proteins produced a toxicity signature of eleven elevated and four attenuated blood protein levels. These blood protein perturbations begin to provide a systems view of key mechanistic features of APAP-induced liver injury relating to glutathione and S-adenosyl-L-methionine (SAMe) depletion, mitochondrial dysfunction, and liver responses to the stress. Two markers, elevated membrane-bound catechol-O-methyltransferase (MB-COMT) and attenuated retinol binding protein 4 (RBP4), report hepatic injury significantly earlier than the current gold standard liver biomarker metric, alanine transaminase (ALT). These biomarkers were perturbed prior to onset of irreversible liver injury. Five of these mouse liver-specific blood markers had human orthologs that were also found to be responsive to human hepatotoxicity. These proteins appear along with conventional biomarkers and non-organ specific potential biomarkers in Figure 14.

A

Symbol	Protein name	Cellular localization	SPRI	WB	MS
ALDH1L1	Aldehyde dehydrogenase 1 family, member L1	Cytoplasm		↑	↑
BHMT	Betaine--homocysteine S-methyltransferase 1	Cytoplasm		↑	↑
CPS1	Carbamoyl-phosphate synthetase 1	Mitochondrion	↑	↑	↑
FAH	Fumarylacetoacetate hydrolase	Cytoplasm		↑	↑
FBP1	Fructose-1,6-bisphosphatase 1	Cytoplasm		↑	
GNMT	Glycine N-methyltransferase	Cytoplasm	↑	↑	↑
HPD	4-hydroxyphenylpyruvate dioxygenase	Cytoplasm		↑	↑
MAT1A	Methionine adenosyltransferase 1	Cytoplasm		↑	
MB-COMT	Membrane-bound Catechol-O-methyltransferase	Membrane		↑	
AGXT	Alanine-glyoxylate aminotransferase	Peroxisome		↑	
DPYS	Dihydropyrimidinase	Cytoplasm	↑	↑	↑
ALDOB	Fructose-bisphosphate aldolase B	Cytoplasm	↑	↑	↑
ASGR1	Asialoglycoprotein receptor 1	Membrane	↑	↑	
ASGR2	Asialoglycoprotein receptor 2	Membrane	↑	↑	↑
ASL	Argininosuccinate lyase	Cytoplasm		↑	↑
HMGCS2	3-hydroxy-3-methylglutaryl-Coenzyme A synthase 2	Mitochondrion	↑	↑	
GOT1 (AST)*	Aspartate transaminase	Mitochondrion	↑	↑	
GPT1 (ALT)*	Alanine transaminase	Cytoplasm		↑	↑
GLUD1*	Glutamate dehydrogenase 1	Mitochondrion		↑	
CP	Ceruloplasmin	Secretory	↓	↓	
PLG	Plasminogen	Secretory	↓	↓	↓
RBP4	Retinol-binding protein 4	Secretory	↓	↓	↓
TF	Transferrin	Secretory	↓	↓	↓
ALB1	Albumin	Secretory	↔	↔	

*Conventional liver function biomarkers.

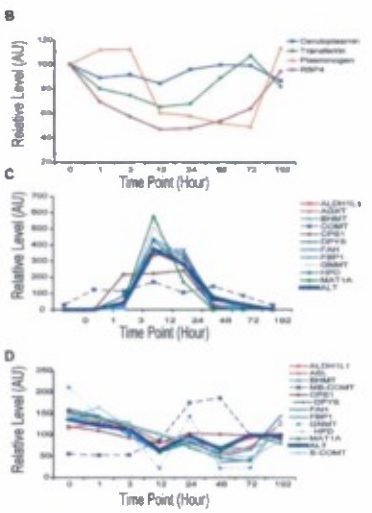

Figure 14. Potential biomarkers observed. A) Using label-free antibody array (SPRI), Western blot (WB), and iTRAQ (MS) methods, 24 protein level changes were observed in mouse plasma. Four proteins are conventional liver function biomarkers and 20 are potentially novel biomarkers. Increased (-), decreased (¯) and unchanged («) measurements are indicated by arrow directions. B) Quantitative plasma profiles for four secretory proteins. C) Quantitative plasma profiles of ALT and novel biomarkers. ALT indicates injury at 3 hours, peak at 12 hours, and return to baseline at 96 hours. ALT levels here were assayed by enzymatic activity and reported in IU/mL. COMT and CPS1 have apparently different patterns from ALT. D) Quantitative liver lysate profiles of the novel blood biomarkers. Lysate profiles differed greatly from the plasma profiles. The increase in COMT levels was shifted later in time, while the other protein levels are attenuated between 24 and 48 hours.

Our *in vivo* experimental approach entailed injecting C57BL/6 mice with half-lethal dose of APAP and then studying the dynamic change of liver-specific protein concentrations in liver and blood. About 30% of the mice died between 24 and 48 hours. Histological staining of the sliced tissue showed progressive necrosis increasing to a maximum at 24 hours post-injection. In surviving mice, the liver histopathology returned to normal between 72-192 hours. Blood ALT/AST levels indicated clear injury starting at 3 hours post-injection, with maximal blood ALT/AST values (>10,000 IU/L) occurring between 12-24 hours, then gradually decreasing to normal levels. Including previously identified blood proteins, 24 proteins were observed to correlate with injury using SPRI microarrays, immunoblotting, and mass spectrometry.

Publications and inventions: This work has been submitted for publication (manuscript draft approved by the DOD). "Blood protein signature for hepatotoxicity—systems strategy for organ-specific biomarker discovery." Zhiyuan Hu, Christopher Lausted, Xiaowei Yan, Hyuntae Yoo, Amy Brightman, and Leroy Hood. (Submitted to Molecular and Cellular Proteomics.)

A patent application has also been filed in the USA and Europe.

- United States Patent Application Serial Number 12/785,279 entitled NEW BIOMARKERS FOR LIVER INJURY, filed 21 May 2010, assigned to the Institute for Systems Biology
- PCT /US2010/035829 entitled NEW BIOMARKERS FOR LIVER INJURY, filed 21 May 2010, assigned to the Institute for Systems Biology.

D. Analysis of the transcriptome after acetaminophen exposure (Kai Wang reporting)

Analysis of mRNA in liver: We conducted detailed studies on the effects of acetaminophen overdose on the transcriptome in mouse liver. Like earlier reports, most of metabolism-related biological processes including pathways associated with lipid, amino acid, carbohydrate, and nucleotide metabolisms are all significantly suppressed in the liver while various cell proliferation and cell signaling pathways were enhanced after acetaminophen overdose (Table 8).

One of the key players in neutralizing the toxic acetaminophen metabolite, N-acetyl-p-benzoquinoneimine is glutathione. In contrast to transcripts involved in other metabolism related pathways, the levels of transcripts encoding enzymes involved in glutathione metabolism, such as various glutathione S-transferases, glutathione reductase and glutathione synthetase are all significantly induced after acetaminophen exposure. This also indicated by the strong enrichment of glutathione metabolism pathway associated with up-regulated genes after acetaminophen overdose (Table 8). This suggests a compensation mechanism in the cells trying to replenish glutathione levels in order to metabolize acetaminophen and its toxic metabolite.

The ability to construct biologically meaningful gene networks and modules from transcriptome studies is critical for contemporary systems biology. We have devised a method, Semantic Similarity-Integrated approach for Modularization (SSIM) that integrates various gene-gene pairwise similarity values, including information obtained from gene expression, protein-protein interactions and GO annotations, in the construction of modules using affinity propagation clustering. In comparison with previously reported algorithms, modules identified by SSIM showed significantly stronger association with biological functions. Specifically, SSIM is effective in identifying coherent functional modules in which genes are highly co-expressed, interconnected via

protein-protein interactions and functionally similar in terms of GO annotations (Figure 15). The SSIM approach can also reveal the hierarchical structure of gene modules to gain a broader functional view of the biological system. Hence, the proposed method can facilitate comprehensive and in-depth analysis of high throughput experimental data at the gene network level.

Category	Pathway Description	Up-regulated				Down-regulated			
		3 hr	8 hr	24 hr	48 hr	3 hr	8 hr	24 hr	48 hr
Metabolism	Drug metabolism other enzymes	3.E-02					9.E-10		
	Metabolism of xenobiotics by cytochroma P450	2.E-02				2.E-11	2.E-21	4.E-05	
	Drug metabolism P450					2.E-12	3.E-23	1.E-05	
	Propanoata matabolism						4.E-02	7.E-02	
	Pantosa and glucuronata interconversions		6.E-02				6.E-03		
	Starch and sucrosa matabolism						4.E-03		
	Ascorbata and aldarata matabolism						3.E-03		
	Butanoata matabolism						1.E-03		
	Fructosa and mannosa matabolism		2.E-02						
	Galactosa matabolism		6.E-02						
	Glycolysis / Gluconaoganasis		8.E-02					8.E-02	
	Pyruvata matabolism		7.E-02						
	Histidina matabolism						1.E-01		
	Selanoamino acid metabolism						8.E-02		
	Phanylalanina matabolism						7.E-02	4.E-02	
	Tyrosina matabolism						3.E-02	2.E-03	
	Cystaina and methionina matabolism						3.E-03		
	Tryptophan matabolism						2.E-03	2.E-02	
	Arginina and proline matabolism						4.E-04	7.E-03	
	Valina, laucina and isolaucina dagradation						2.E-05		
	Alanina, aspartata and glutamata matabolism						3.E-06		
	Glycina, sarina and thraonina matabolism						6.E-07	1.E-02	
	beta-Alanina metabolism						7.E-02		
	Glutathiona matabolism	1.E-04	5.E-04	4.E-03	8.E-02				
	Staroid biosynthesis					6.E-03	4.E-02	3.E-11	1.E-01
	Eatty acid biosynthesis						3.E-02	9.E-02	
	Biosynthesis of unsaturatad fatty acids						6.E-03	6.E-02	
	Primary bila acid biosynthasis					5.E-03	3.E-04		
	Androgen and astrogen matabolism						7.E-05	8.E-02	
	Arachidonic acid metabolism					4.E-09	2.E-06		
	Staroid hormone biosynthasis						3.E-11	5.E-04	
	Linolaic acid matabolism					7.E-10	1.E-14	3.E-02	
	Purina matabolism		5.E-02						
	Pyrimidina matabolism		2.E-02						
	Sulfur matabolism						7.E-02	9.E-03	
	Nitrogen metabolism						4.E-04	4.E-02	
	Porphyrin and chlorophyll metabolism						4.E-02		
	Pantothanata and CoA biosynthesis						3.E-02		
	Ratinol matabolism					2.E-11	2.E-16	6.E-06	
	Tarpenoid backbona biosynthasis					1.E-04	2.E-04	1.E-06	
Signaling and cell growth	MAPK signaling pathway			4.E-04	4.E-07				
	ECM-racaptor interaction	4.E-02	6.E-03						
	Cell cycla	2.E-06	9.E-10	7.E-02					
	Oocyta maiosis	1.E-05	5.E-05						
	p53 signaling pathway	4.E-04	1.E-02	5.E-02	3.E-03				
	Pathways in cancar		3.E-02		7.E-02				
	PPAR signaling pathway						2.E-02		
	Progastarona-madiatad oocyta maturation	1.E-04	7.E-03						
	Ribosoma		1.E-17						
	Basa axcision rapair		7.E-02						
	DNA raplication		2.E-09						
	Homologous recombination		2.E-02						
	Mismatch rapair		6.E-03						
	Nuclaotida axcision rapair		9.E-02						
	Regulation of actin cytoskalaton		3.E-02						
	Focal adhasion	2.E-03	5.E-02						
	Gap junction		2.E-04						
Immune response	Complamant and coagulation cascadas						2.E-03		
	Toll-lika racaptor signaling pathway				6.E-02				

Table 8. Molecular pathways in liver affected by acetaminophen overdose. The p values were calculated by Database for Annotation, Visualization and Integrated Discovery (http://david.abce.neifcrf.gov/home.jsp).

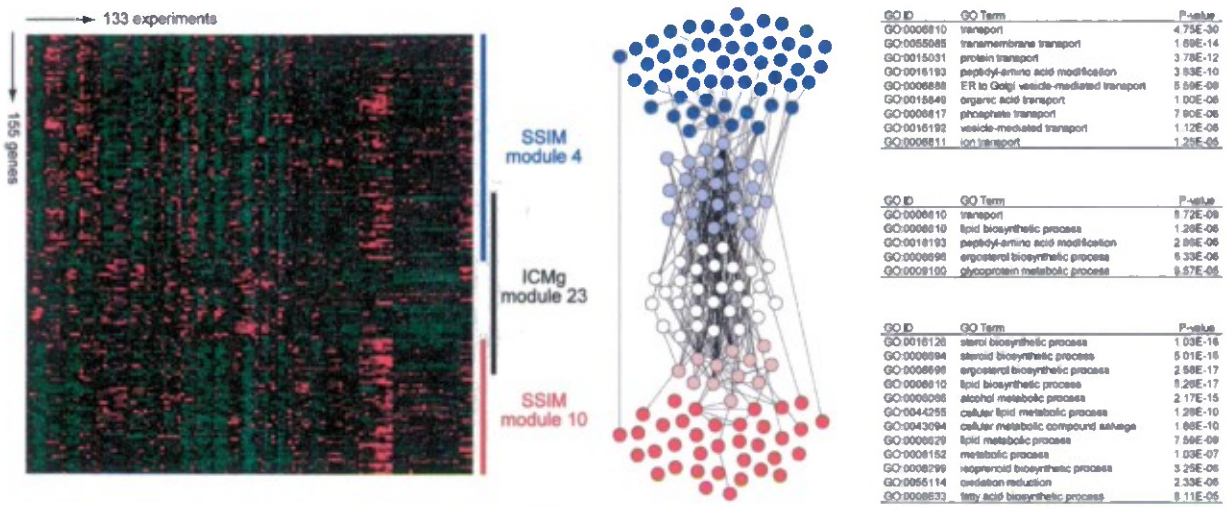

GO ID	GO Term	P-value
GO:0006810	transport	4.75E-30
GO:0055085	transmembrane transport	1.69E-14
GO:0015031	protein transport	3.78E-12
GO:0018193	peptidyl-amino acid modification	3.83E-10
GO:0006888	ER to Golgi vesicle-mediated transport	5.59E-09
GO:0015849	organic acid transport	1.00E-08
GO:0006817	phosphate transport	7.90E-08
GO:0016192	vesicle-mediated transport	1.12E-08
GO:0006811	ion transport	1.25E-08

GO ID	GO Term	P-value
GO:0006810	transport	8.72E-09
GO:0008610	lipid biosynthetic process	1.26E-08
GO:0018193	peptidyl-amino acid modification	2.89E-08
GO:0006696	ergosterol biosynthetic process	5.33E-08
GO:0009100	glycoprotein metabolic process	9.57E-08

GO ID	GO Term	P-value
GO:0016126	sterol biosynthetic process	1.03E-16
GO:0006694	steroid biosynthetic process	5.01E-16
GO:0006696	ergosterol biosynthetic process	2.58E-17
GO:0008610	lipid biosynthetic process	9.29E-17
GO:0006066	alcohol metabolic process	2.17E-15
GO:0044255	cellular lipid metabolic process	1.29E-10
GO:0043094	cellular metabolic compound salvage	1.68E-10
GO:0006629	lipid metabolic process	7.56E-09
GO:0008152	metabolic process	1.03E-07
GO:0008299	isoprenoid biosynthetic process	3.25E-06
GO:0055114	oxidation reduction	2.33E-06
GO:0006633	fatty acid biosynthetic process	8.11E-05

Figure 15. Comparison between modules identified by ICMg and SSIM. One of the modules identified by ICMg method (ICMg module) shares a number of genes with two separate modules identified by SSIM (SSIM module A and B). Expression profiles of genes in three modules are shown on the left and protein-protein interaction network are shown in the middle. Genes shared by ICMg and SSIM modules are indicated by pink and light blue nodes, and ones exclusively belong to ICMg, SSIM module A and SSIM module B are depicted by white, red and blue nodes, respectively. In the right panel, enriched GO BP terms ($p<1\times10\text{-}5$) and their uncorrected p-values for each module are summarized (adapted from Cho et al 2011 *BMC Systems Biology)*

Analysis of mRNA transcripts in blood: Several reports have been described the possibility of using the levels of liver-specific transcripts in plasma as biomarkers to reflect the pathological conditions in the liver. We adapted the NextGen sequencing technology to conduct a detailed characterization of normal plasma RNA spectrum as well as the effect of acetaminophen overdose on the circulating RNAs. This would allow us to explore the complexity of RNA spectrum in plasma, aid our understanding on the effect of acetaminophen overdose, and identify more informative biomarker for liver injury. Because of the low RNA concentration in the plasma, we made some modifications in the sequencing library preparation protocol. With the modified protocol, we obtained about 28 million reads from each sample, after trimmed the adaptors, and removed low quality, polyA only and adaptor only sequences, we obtained about 2 to 9 millions of processed reads from our plasma samples.

Besides the significant changes on miR-122 and miR-192 levels, similar to what we reported earlier (Wang et al 2009 PNAS) and described below, we also observed a significant increase of several liver-specific mRNAs including albumin (Alb), ferritin (Fth1) and apolipoprotein A2 (Apoa2) (Figure 16). We are in the process of conducting a more detailed analysis on the sequence data and prepare a manuscript to report the finding.

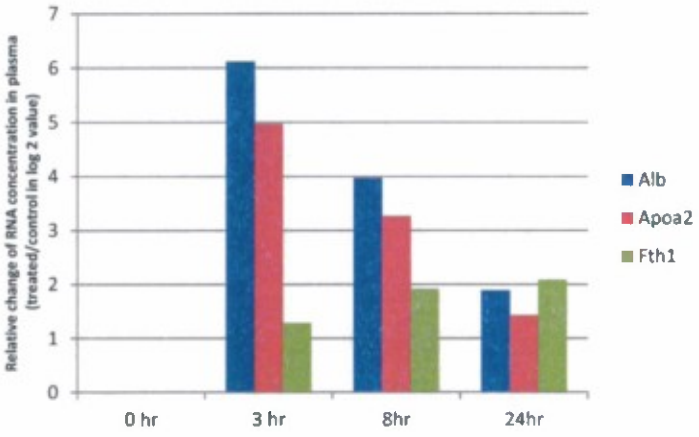

Figure 16. The changes on the levels of several liver specific genes in plasma. The Y-axis is the changes on the number of reads in log 2 value between treated vs. control and individual time points post acetaminophen exposure are indicated on the X-axis. The gene identity is listed on the right of the figure.

Analysis of microRNA: MicroRNAs (miRNAs) are 19-23 nucleotides, non-coding regulatory RNAs in the cells. With support from DOD, we also pioneered the use of miRNA in toxicology. Using the acetaminophen overdose animal model, we demonstrated that levels of circulating liver enriched microRNAs, miR-122 and miR-192 are far more sensitive than traditional serological aminotransferase markers (Figure 17).

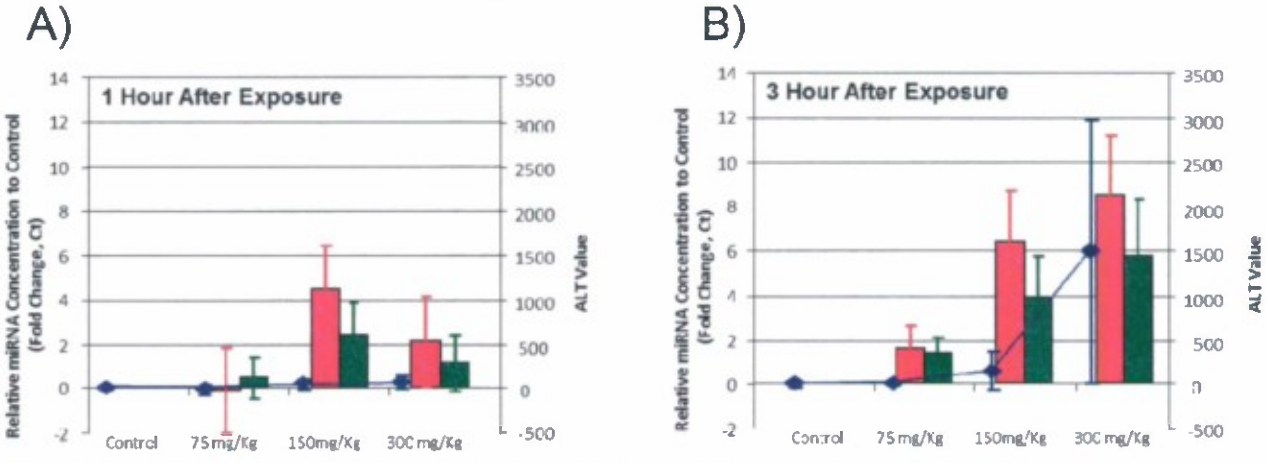

Figure 17. microRNA are more sensitive markers than SGPT for liver injury Comparison between the levels of mir-122 (red bars), mir-192 (green bars) and SGPT (blue line) in plasma samples collected from mice 1 (A) and 3 hours (B) after exposed to different doses of acetaminophen (indicated on X-axis). The relative change of miRNA expression levels (ratio in log 2 compare to control) is indicated on the left side of the figure and the scale of SGPT level is on the right. The relative change of miRNA levels are expressed in log 2 ratio of each treatment condition compared to the corresponding control. Values of miRNA fold change and SGPT levels are the average of 4 independent samples from each time point and the standard derivations are shown as error bars. (adapted from *Wang et al 2009 PNAS*)

This finding was reported in a publication by Wang et al in 2009. Most of the pharmaceutical companies are now using the level of miR-122 in circulation as routine screen in their therapeutics development pipeline.

To broaden the utility of using miRNA as biomarker, we also profiled the miRNA composition of 12 different types of body fluids including amniotic fluid, breast milk, bronchial lavage, cerebrospinal fluid, colostrum, peritoneal fluid, plasma, pleural fluid, saliva, seminal fluid, tears, and urine to gain a better understanding on the distribution and composition of miRNA in different body fluids. (Figure 18). Some of the miRNAs in urine are actually associated with different pathological conditions. This suggested the possibility of using miRNA as biomarker for various physio-pathological conditions.

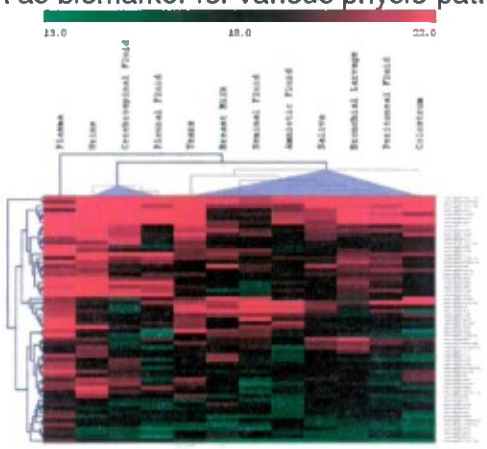

Figure 18. The body fluid types can be grouped into two major clusters based on the profile of commonly expressed miRNAs. Unsupervised hierarchical clustering on commonly "expressed" miRNAs groups the samples into two major groups. Plasma is separated from the two major clusters (adapted from *Weber et al. 2010 Clinic Chem*)

The ideal biomarker should fit a number of criteria depending on how the biomarker is to be used (Table 9, adapted from *Etheridge et al 2011 Mutation Res*). It should be accessible through non-invasive methods, specific to the disease or pathology of interest, a reliable indication of disease before clinical symptoms appear (early detection), sensitive to changes in the pathology (disease progression or therapeutic response), and easily translatable from model systems to humans. miRNAs are stable in various bodily fluids, the sequences of most miRNAs are conserved among different species, the expression of some miRNAs is specific to tissues or biological stages, and the level of miRNAs can be easily assessed by various methods, including methods such as polymerase chain reaction (PCR), which allows for signal amplification.

Specific
Specific to diseased organ or tissue
Able to differentiate pathologies
Sensitive
Rapid and significant release upon the development of pathology
Predictive
Long half-life in sample
Proportional to degree of severity of pathology
Robust
Rapid, simple, accurate and inexpensive detection
Unconfounded by environment and unrelated conditions
Translatable
Data can be used to bridge pre-clinical and clinical results
Non-invasive
Present in accessible fluid sample

Table 9. Characteristics of an ideal biomarker.

It has been shown that some miRNAs frequently have sequence variations termed isomirs. To better understand the extent of miRNA sequence heterogeneity and its potential implications for miRNA function and measurement, we conducted a comprehensive survey of miRNA sequence variations from human and mouse samples using next generation sequencing platforms. Our results suggest that the process of generating this isomir spectrum might not be random and that heterogeneity at the ends of miRNA affects the consistency and accuracy of miRNA level measurement. In addition, we have constructed a database from our sequencing data that catalogs the entire repertoire of miRNA sequences (http://galas.systemsbiology.net/cgi-bin/isomir/find.pl) (Figure 19). This enables users to determine the most abundant sequence and the degree of heterogeneity for each individual miRNA species. This information will be useful both to better understand the functions of isomirs and to improve probe or primer design for miRNA detection and measurement (Lee et al 2010 *RNA*)

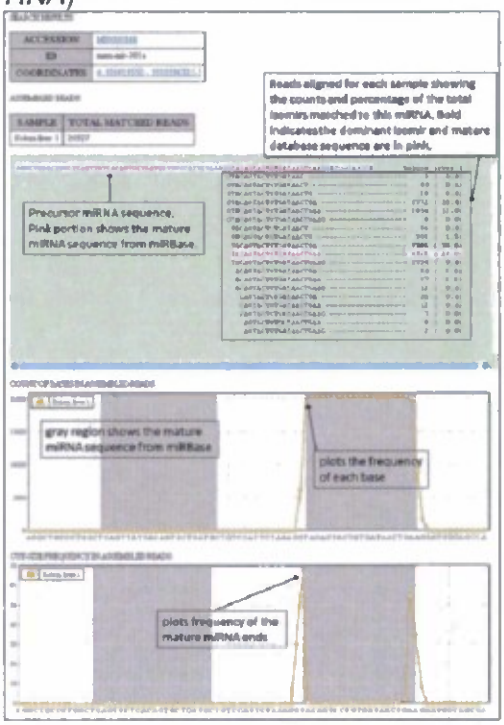

Figure 19. A screen shot of isomir database. The aligned reads and corresponding counts are shown. The first plot shows the frequency of the bases and the second plot shows the frequency of the mature miRNA end positions. Sequences that match perfectly to miRBase sequences are shown in pink and most abundant sequence are displayed in bold (adapted from Lee et al 2010 RNA).

Publications and inventions:

Wang, K., Zhang, S., Marzolf, B., Troisch, P., Brightman, A., Hu, Z., Hood, L. and Galas, D. J. (2009) Circulating microRNAs, a new class of blood biomarker for drug-induced liver injury. *Proc. Natl. Acad. Sci. USA.* 106 4402-4407

Weber, J., Baxter, D., Zhang, S., Huang, K. H., Lee, M. J., Galas, D. J. and Wang, K. (2010) The microRNA spectrum in 12 body fluids. *Clin Chem.* 56:1733-41.

Lee, L. W., Etheridge, A., Zhang S., Ma, L., Martin, D., Galas, D. J. and Wang, K. (2010) Complexity of the microRNA repertoire revealed by next-generation sequencing. *RNA*. 16:2170-80.

Cho, J. H., Wang, K., and Galas, D. J. (2011) An integrative approach to construct biologically meaningful modules. *BMC Systems Biology*, 26:117-126.

Etheridge, A., Lee., I. Y., Hood, L. E., Galas, D., and Wang, K. (2011) Extracellular microRNA: a new source of biomarkers. *Mutation Res*. 717:85-90.

Patent:
Methods, compositions, and devices utilizing microRNA to determine physiological conditions. Application Number:12/615969

VX studies

Aim 5: Analyze time course experiments of rat tissues and blood exposed to VX.
Yong Zhou and Kai Wang reporting

Introduction: The lethal contact nerve agent, VX (S-(diisopropylaminoethyl) methylphosphonothiolate o-ethyl ester) (Figure 20) is a potent organophosphate that inhibits acetylcholinesterase (AChE), an enzyme responsible for the breakdown of the neurotransmitter acetylcholine (ACh). The accumulation of excessive ACh at synapses causes overstimulation of the neuromuscular junction that controls smooth muscle, cardiac muscle, and exocrine glandular function. VX is more stable, more resistant to detoxification, more efficient at skin penetration, and more environmentally persistent compared to other organo-phosphate nerve gas compounds.

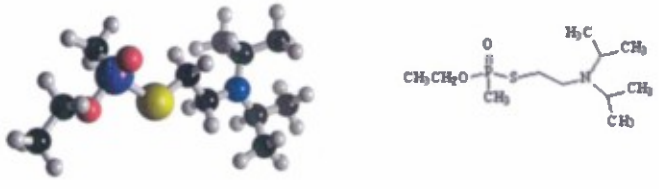

Figure 20. The chemical structure of VX. The space filling model is shown on the left while the chemical structure is on the right.

Although blood cholinesterase (ChE) activity has been used as an indicator of nerve agent exposure or as an index of recovery, the measurement suffers from extensive measurement background. In addition, the high variability of normal blood ChE activity makes it difficult to use blood ChE activity as a reliable indicator for organophosphate exposure. To further understand the mechanisms of VX induced toxicity and identify more reliable candidate blood biomarkers of VX exposure and recovery, since 2009, scientists at ISB have been collaborating with Dr. Jennifer Sekowski at Edgewood Chemical Biological Center (ECBC) to perform systems biological studies on rat tissues and plasma exposed to VX. Overall, we received samples from 23 VX-treated rats (subcutaneous injection at 80% LD_{50} dosage, 12 μg/kg) and 16 control rats. Time-course serum samples were collected before treatment ('pre') and at 2 hours, 24 hours, 48 hours, and 72 hours post-exposure, respectively, while brain and liver samples were also collected at 72 hours post-exposure.

Proteome studies of rat brain tissue exposed with VX Nerve Gas: First, quantitative global proteomic analyses were conducted in cerebellum and cerebrum regions, respectively by quantifying the relative abundances of proteome in 4 VX-treated and 4

control rat cerebellum/cerebrum samples through labeling tryptic peptides with 8-plex iTRAQ reagents and conducting LC-MS/MS analyses.

These two proteomic experiments revealed relative quantification of approximately 1,000 proteins in both brain regions. Interestingly, only two proteins, GFAP (Glial fibrillary acidic protein) and SPTBN2 (spectrin, beta, non-erythrocytic 2) showed statistically significant differences ($p < 0.05$) —a reduction in VX-treated cerebellum (Figures 21B and 22B) but not in cerebrum (Figure 24). Western Blot experiments on the same rat cerebellum samples confirmed the downtrend of GFAP but not SPTBN2 (Figures 21A and 22A).

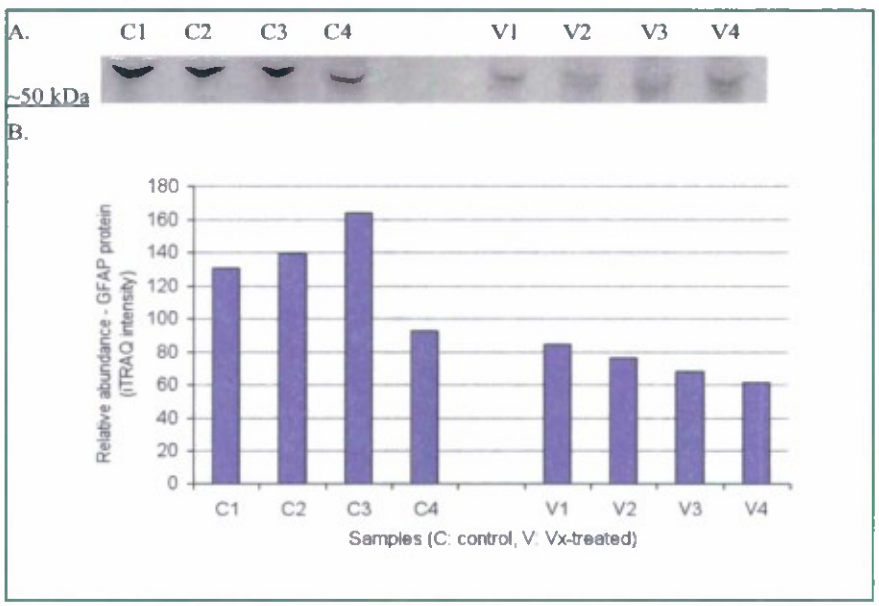

Figure 21. Abundance of GFAP in cerebellum of control and VX-treated rats, as measured by Western Blot (A) and iTRAQ-based proteomic analysis (B), respectively.

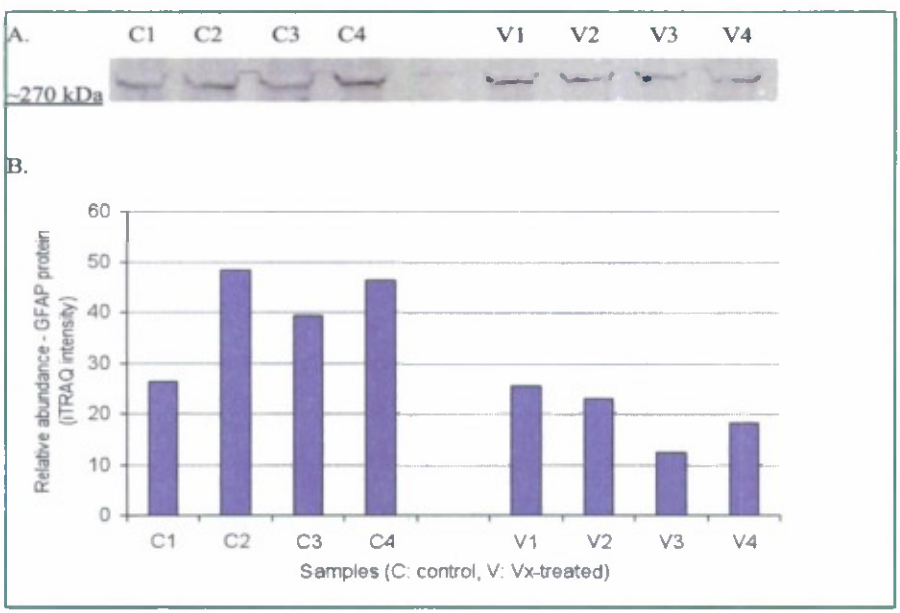

Figure 22. Abundance of SPTBN2 in cerebellum of control and VX-treated rats, as measured by Western Blot (A) and iTRAQ-based proteomic analysis (B), respectively.

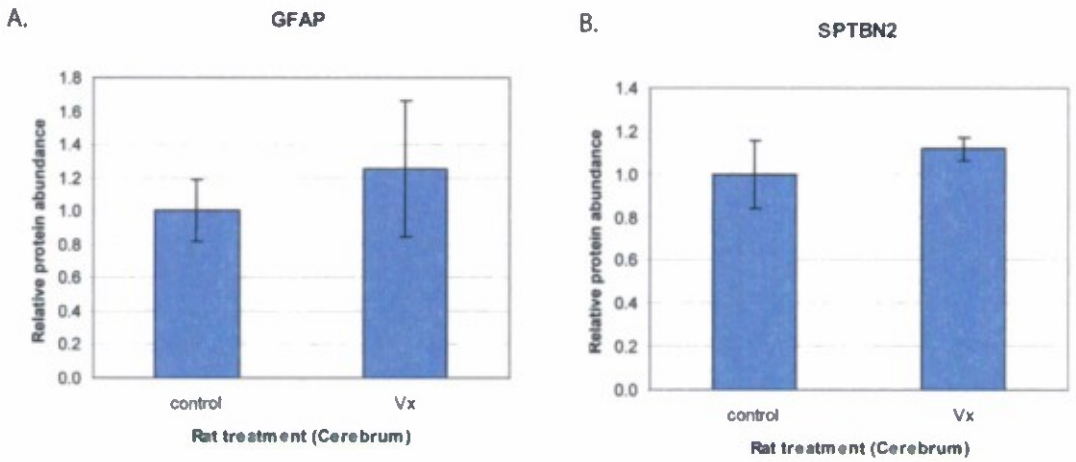

Figure 23. Differences in levels of GFAP and SPTBN2 in cerebrum samples of rats treated with saline (control) or VX. Error bars represent standard errors among biological replicates (n=4), $p > 0.4$ for both GFAP and SPTBN2.

Circulating microRNAs in animals exposed with VX Nerve Gas: To determine whether circulating miRNA can also be used as more reliable biomarkers for organophosphate exposure, we also did an initial survey of circulating miRNA spectra from time-course VX exposed rat serum (control, 2 hr, 24 hr, 48 hrs and 72 hrs post exposure).

The amount of total RNA extracted from pooled serum samples ranges from 950 to 1600 ug/ml and the estimated miRNA population ranges from 460 to 1150 ug/ml based on the results from Agilent 2100 Bioanalyzer (Figure 25). There is a gradual decrease on the amount of total RNA as well as miRNA in the blood post VX exposure. This may indicate severe and persist injury after VX exposure after 48 hours; however, more detailed pathological information is needed in order to draw any conclusions on the decrease of RNA levels. There is a sudden decrease of RNA and miRNA levels 2 hrs post exposure, which may have resulted from acute injuries or responses from the animals toward VX exposure.

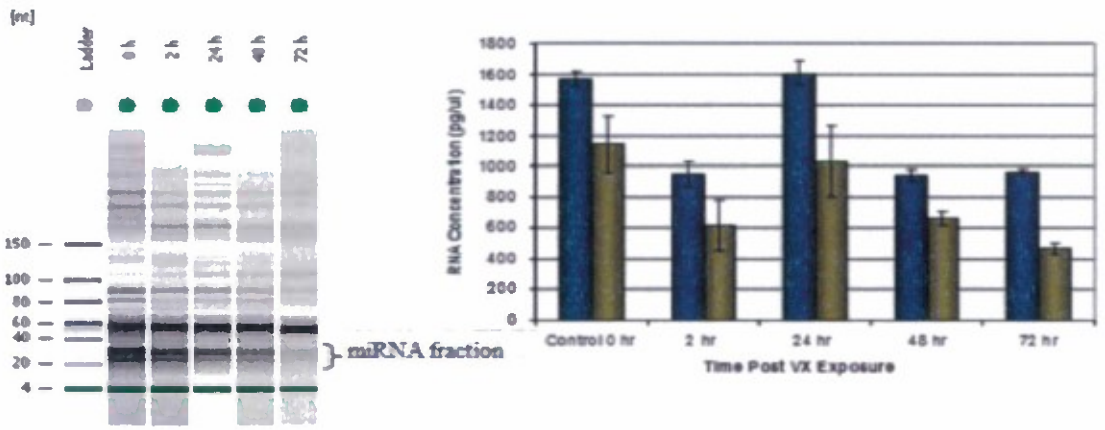

Figure 24. The quality of quantity of RNA isolated from VX exposed serum samples. The image from Bioanalyzer 2100 is shown on the left the RNA (blue bars) and estimated microRNA (yellow bars) concentrations are shown on the right. The RNA and miRNA concentrations were obtained from two independent measurements. The size range used to estimate miRNA concentration is labeled on the Bioanalyzer image.

By using a low-density taqman card, we have identified 62 circulating miRNAs that are detectable in all the samples except those from 72 hrs post exposure. Thirty-nine of them displayed significant changes during the course of the experimental period (Figure 25). Similar as the concentrations of blood total RNA, the specific miRNA levels also gradually decreased after VX exposure. Several miRNAs, including mir-128s, mir-27b, mir-15b and mir-let7e, showed a significant decrease during the first two hours of VX exposure. These may have great potential to be used as a signature for VX or general organophosphate exposure. More samples with different organophosphate compounds are needed in order to determine the specificity and sensitivity of these circulating miRNAs for VX exposure.

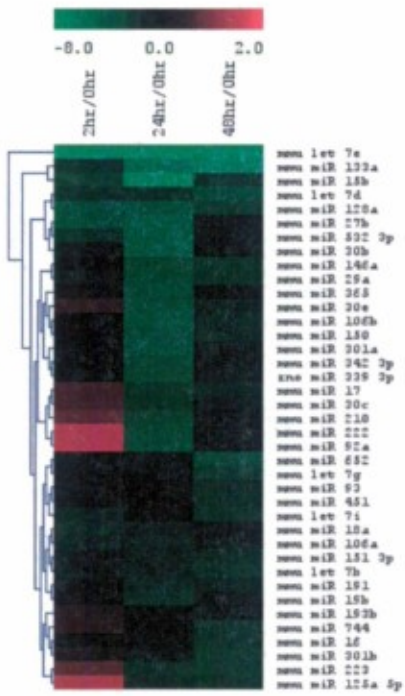

Figure 25. Hierarchical cluster analysis of 39 differentially expressed miRNA in VX exposed serum relative to control. The identities of miRNAs are shown on the right and the samples are indicated on the top.

The most affected miRNA species from VX exposure are mir-let 7e and mir-133a. The decrease of mir-133 is especially interesting since it is a miRNA that is highly enriched in muscles. VX has a well-known, severe effect on the muscle, which may cause the decrease of mir-133a (Fig 26A). Unlike the mir-133a, there are several miRNAs that showed an initial decrease followed by a gradual recovery, such as the mir-30s (Fig 5-7B). This may suggest the recovery of some biological functions after initial VX exposure; however, more pathological information is needed to understand the recovery of certain miRNA species in the blood. We failed to detect brain specific miRNAs, such as mir-124 in the blood, which may indicate that the VX nerve toxin did not cause significant structural damage on the CNS.

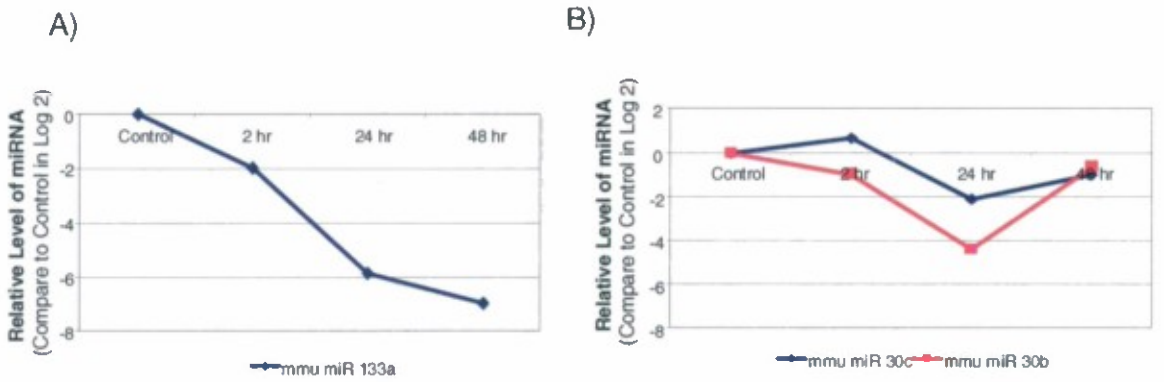

Figure 26. Relative miRNA changes, compared to controls, in the experimental period. The mir-133a shows a gradual decrease (A) while the mir-30s (B) regain their normal levels 48 hours after VX exposure.

The changes in the spectrum of circulating microRNA (miRNA) in blood correlate well with various physiopathological conditions including cancers, cardiovascular conditions and liver injuries. These observations clearly suggest that the spectrum of extracellular blood miRNA can be used as informative biomarkers to monitor the body's physiopathological status. Unlike protein-based markers, detecting specific miRNA species in the blood is a much easier task in general.

Quantitative mapping of serum proteome in VX gas exposed rats: Our goals of serum proteome profiling include 1) to test the hypothesis that the serum proteome contains signals that correlated to VX exposure over time course (from 0h to 72h), 2) to identify putative biomarkers for VX exposure and recovery, 3) to further understand the mechanisms and targets of VX-induced toxicity. Considering the complexity of serum proteome, high dynamic range of serum proteins, and the difficulties in analyzing proteomics data with multiple time points, we adapted an approach by combining affinity column to deplete high abundant plasma proteins with high resolution and high sensitivity mass spectrometry to conduct label-free quantitative proteomic analyses. In order to be comparable with microRNA profiling data, the same, pooled serum sample set was used in the proteome profiling experiment.

By using this approach, from a set of five pooled VX-treated rat sera (15 µl each), we identified 3,189 unique peptides from 233 distinct proteins with ProteinProphet cut-off score of ≥0.7 and error rate <0.05. The average peptide sequence coverage is about 15.0%. Although the majority of identified proteins are well-known highly abundant serum proteins, a number of tissues derived proteins are also identified. For example, the vesicle-associated membrane proteins 1 (Vamp1), dendrin (Ndn), periaxin (Prx), and solute carrier family 5 (choline transporter) (Slc5a7) are cytoplasm/membrane proteins that highly expressed in brain.

In the label-free proteomics analysis, 7,231 features were aligned with minimum of 3 LC-MS runs. The scatter plots (Figure 27) clearly describe that hundreds of features are either up- or down- presented at 24h and 48h post VX exposure. Although the majority of these changes are not statistically significant due to the small sample size, this phenomenon is still encouraging. Meanwhile, considering that the intensities of same features in duplicate runs at the same time point are more consistent comparing to that at different time points, the variations presenting at 24h and 48h are likely to be from the samples.

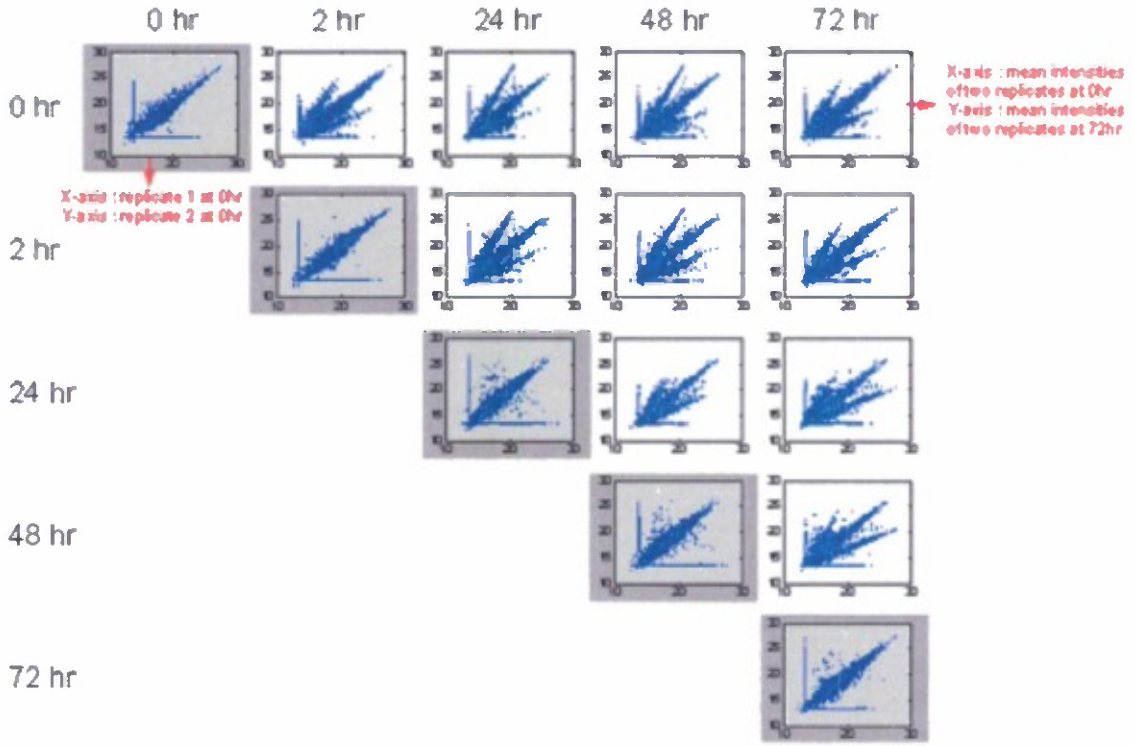

Figure 27: Aligned feature intensity comparisons between VX-treatment time points. Scatter plots are either between two replicates at the same time point (gray shaded), or between mean intensities of two different time points (off-diagonal)

By adapting time-course statistic tools like EDGE (Extraction of Different Gene Expression), we identified 63 proteins that showing significant changes on their levels in blood during VX exposure (Table 10). Interestingly, 22 of them have been reported previously as inflammatory response- and/or acute-phase- associated plasma proteins, which further suggest the involvement of inflammatory processes in VX induced injury. For example, the ITIH4 (inter-alpha-trypsin inhibitor heavy chain 4) has been identified as an acute-phase protein isolated from cattle during experimental infection with a mixture of *Actinomyces pyogenes*, *Fusobacterium necrophorum*, and *Peptostreptococcus indolicus* (M. Piñeiro, et al, *Infection and Immunity*, 2004, Vol. 72, p 3777-3782).

On the other hand, 8 liver-specific proteins are presenting in the differential expressed protein list. The changes of these liver enriched proteins clearly suggest the involvement of liver in VX induced toxicity. For example, carboxylesterase 1 precursor (CES1), a liver-specific intracellular membrane protein that involves in the detoxification of xenobiotics and in the activation of ester and amide prodrugs, were suppressed after 24 hours of VX exposure, which may indicate close association of CES1 in VX metabolism.

Gene Symbol	Protein Description	*VX0h*	*VX2h*	*VX24h*	*VX48h*	*VX72h*	*P-Value*	*Q-Value*	Inflammatory/Acute phase *
Afm	afamin	0	-0.1899	-0.4208	-0.2393	-0.9850	*0.0118*	*0.1169*	
Ahsg	alpha-2-HS-glycoprotein	0	0.0804	0.5875	0.5217	0.2555	*0.0367*	*0.1386*	Yes
Alb	albumin	0	0.1133	1.0945	0.4803	0.0170	*0.0004*	*0.0157*	
Apoa1	apolipoprotein A-I	0	-0.2064	-0.3466	-0.1566	-0.6569	*0.0379*	*0.1395*	
Apoa4	apolipoprotein A-IV	0	0.1177	-0.0527	-0.1849	-0.2471	*0.0170*	*0.1169*	
Apob	apolipoprotein B	0	-0.9853	-0.9146	-0.8583	-10.7983	*0.0000*	*0.0006*	
Apoe	apolipoprotein E	0	0.1555	-0.4810	-0.3931	-0.6985	*0.0210*	*0.1169*	
Apoh	apolipoprotein H	0	0.5107	0.9790	0.7262	0.7313	*0.0190*	*0.1169*	
Apom	apolipoprotein M	0	0.0107	-0.2633	-0.1616	-0.2565	*0.0413*	*0.1452*	
C2	complement component 2	0	0.0662	0.6389	0.7299	0.5742	*0.0196*	*0.1169*	Yes
C3	complement component 3	0	0.0932	0.2772	-0.2338	-0.4614	*0.0218*	*0.1169*	Yes
C9	complement component 9	0	0.4811	1.1476	0.6213	0.7258	*0.0349*	*0.1356*	Yes
Cfh	**complement component factor H**	0	**0.6312**	**2.3729**	**1.4048**	**2.0601**	**0.0049**	**0.1035**	**Yes**
Cfi	complement factor I	0	0.7813	1.4797	1.2300	1.2613	*0.0119*	*0.1169*	Yes
Cfp	complement factor properdin	0	-0.0144	-0.2274	-0.4097	-0.6290	*0.0146*	*0.1169*	Yes
Clu	clusterin	0	0.1142	-0.4377	-0.3554	-0.5143	*0.0250*	*0.1169*	Yes
Cp	ceruloplasmin	0	0.6883	2.1067	1.3146	1.5143	*0.0011*	*0.0329*	
Cpn1	**carboxypeptidase N, catalytic chain**	0	**-0.1075**	**-0.4720**	**-0.2857**	**-0.5282**	**0.0241**	**0.1169**	
D3ZC54_RAT	Uncharacterized protein	0	-0.1707	-0.1245	-5.4128	-10.4865	*0.0259*	*0.1169*	
D4AC77_RAT	Uncharacterized protein	0	0.1481	-0.2754	-9.8188	-1.1309	*0.0002*	*0.0109*	
Es1	**esterase 1**	0	**-0.1575**	**-0.6346**	**-0.4511**	**-0.4119**	**0.0037**	**0.0932**	
F2	coagulation factor II	0	0.9298	2.4570	2.8775	2.3656	*0.0444*	*0.1519*	Yes
Fetub	fetuin beta	0	0.7428	2.7018	2.0964	2.1106	*0.0002*	*0.0109*	
Fga	fibrinogen, alpha polypeptide	0	0.3692	1.7791	0.9855	1.0976	*0.0099*	*0.1169*	
Fgb	fibrinogen, B beta polypeptide	0	0.4264	1.9615	1.0351	1.1902	*0.0186*	*0.1169*	
Fgg	fibrinogen, gamma polypeptide	0	0.4821	1.5807	0.5478	1.1169	*0.0240*	*0.1169*	
Fn1	fibronectin 1	0	0.5184	1.4067	0.2692	1.0195	*0.0048*	*0.1033*	Yes
Gc	group specific component	0	-0.0692	-0.9088	-0.4078	-0.6824	*0.0160*	*0.1169*	
Gsn	gelsolin	0	3.5089	8.9027	7.9854	8.3943	*0.0206*	*0.1169*	
Hbb	hemoglobin, beta	0	-0.3067	-0.4307	-0.4960	-1.8646	*0.0170*	*0.1169*	
Hp	haptoglobin	0	0.2375	0.8476	0.1169	0.2776	*0.0038*	*0.0932*	
Hps5; Saa4	Hermansky-Pudlak syndrome 5	0	0.5478	2.8935	-7.7999	-2.8250	*0.0456*	*0.1542*	
Hpx	hemopexin	0	0.0924	1.7479	0.7231	0.9171	*0.0140*	*0.1169*	
Hrg	**histidine-rich glycoprotein**	0	**0.6258**	**2.2868**	**2.1702**	**1.9479**	**0.0004**	**0.0181**	
Igh-1a	IgG heavy chain 1a (serum IgG2a)	0	0.2443	1.0688	-0.1614	0.5514	*0.0186*	*0.1169*	
Itih1	inter-alpha trypsin inhibitor, heavy chain 1	0	0.0239	-0.2731	-0.7616	-0.1865	*0.0066*	*0.1169*	
Itih3	**inter-alpha trypsin inhibitor, heavy chain 3**	0	**0.2360**	**0.6870**	**0.2759**	**0.3053**	**0.0366**	**0.1386**	
Itih4	**inter alpha-trypsin inhibitor, heavy chain 4**	0	**-0.1000**	**-0.3499**	**-0.1456**	**-0.5120**	***0.0240***	***0.1169***	**Yes**
Kng2	kininogen 2	0	0.4059	2.0760	1.1404	1.4665	*0.0063*	*0.1169*	
LOC297568	alpha-1-inhibitor III	0	-0.1183	-0.3144	-0.1829	-0.6539	*0.0001*	*0.0068*	Yes

LOC299282	Serine protease inhibitor	0	-0.2560	-0.4686	-0.2345	-0.5014	0.0083	0.1169	
LOC360504	hemoglobin alpha 2 chain	0	-0.2225	-0.3069	-0.1715	-1.1911	0.0292	0.1218	
LOC498793	inter-alpha-inhibitor H2 chain	0	-0.1179	-0.1901	-0.3442	0.0429	0.0235	0.1169	
MGC108747	similar to alpha-1 major acute phase protein prepeptide	0	0.2751	0.1718	-0.5375	-0.3147	0.0393	0.1416	Yes
Mug1	Murinoglobulin 1 homolog	0	-0.4060	-1.3770	-0.6357	-1.3577	0.0018	0.0488	
Mug2	murinoglobulin 2	0	0.0380	1.6785	1.7924	1.4022	0.0039	0.0947	
Nfkbil2	nuclear factor of kappa light polypeptide gene enhancer in B-cells inhibitor-like 2	0	0.9788	1.8048	1.9983	1.7982	0.0217	0.1169	Yes
Orm1	orosomucoid 1	0	0.0723	2.1272	0.7767	1.2284	0.0124	0.1169	Yes
Pf4	platelet factor 4	0	-0.1160	0.0309	-0.5258	-0.7967	0.0338	0.1335	
Plg	plasminogen	0	0.3908	1.8879	1.8390	1.5486	0.0049	0.1035	
Pzp	preg20000cy-zone protein	0	-0.0047	0.2190	-0.9434	-0.5315	0.0187	0.1169	
RGD1309019	similar to Ras GTPase-activating protein nGAP (RAS protein activator like 1)	0	-0.4546	-1.1836	-0.2645	-0.7542	0.0291	0.1216	
Serpina1	serine (or cysteine) proteinase inhibitor, clade A, member 1	0	0.0539	1.6327	0.9244	1.0056	0.0245	0.1169	Yes
Serpina10	serine (or cysteine) peptidase inhibitor, clade A, member 10	0	-0.5708	-10.0944	-0.2797	-5.3584	0.0000	0.0006	
Serpina3k	serine (or cysteine) peptidase inhibitor, clade A, member 3K	0	-0.1347	-0.3371	-0.1116	-0.5525	0.0017	0.0488	Yes
Serpina3m	serine (or cysteine) proteinase inhibitor, clade A, member 3M	0	-0.2254	-0.5507	-0.3047	-0.3596	0.0069	0.1169	Yes
Serpina3n	**serine (or cysteine) peptidase inhibitor, clade A, member 3N**	0	**0.3991**	**2.2099**	**1.4240**	**1.7527**	**0.0058**	**0.1156**	**Yes**
Serpina6	serine (or cysteine) peptidase inhibitor, clade A, member 6	0	-0.0028	-0.5596	-0.3196	-0.5268	0.0018	0.0488	
Serpinf2	serine (or cysteine) peptidase inhibitor, clade F, member 2	0	0.9135	2.2223	1.6176	1.8295	0.0043	0.0956	Yes
Serping1	**serine (or cysteine) peptidase inhibitor, clade G, member 1**	0	**0.8368**	**1.5576**	**1.4403**	**1.2841**	**0.0344**	**0.1348**	**Yes**
Srprb	signal recognition particle receptor, B subunit	0	-0.1772	-0.4159	-0.4854	-0.9634	0.0000	0.0006	
Tf	Serotransferrin	0	0.0891	1.3489	1.4019	0.9879	0.0105	0.1169	Yes
Ttr	transthyretin	0	-0.2240	-0.4493	-0.4808	-0.6215	0.0069	0.1169	

Table 10. List of 63 proteins that differentially expressed in VX-exposed rat serum vs. control

Twenty-two of them are inflammatory and acute phase response proteins and 8 are liver-specific proteins (in **Bold**). Differentially expressed proteins were identified by EDGE time-course analysis mode. Select Q-Value cut-off: 0.05, equals to expected false discovery rate: 3.0%.

*: Data from "Dissecting the human plasma proteome and inflammatory response biomarkers" (Chen, et al., Proteomics, 2009, 9, 470-484) and other literatures.

Summary: Under the current contract, scientists at ISB have conducted multiple systems biological analyses in time course experiments of rat tissues and blood exposed to VX and observed that:

1. A proteomics analysis of two brain regions (cerebellum and cerebrum) revealed a reduction in cerebellum glial fibrillary acidic protein (GFAP) at 72 hrs.

2. miRNA analysis demonstrated an elevated level of mir-133a in VX-exposed serum, which is preferentially expressed in muscle tissue.

3. Proteomic analysis of the blood serum unveiled 63 proteins that showing significant changes in serum during VX exposure. Twenty-two of them have been reported previously as inflammatory response- and/or acute-phase- associated plasma proteins. And 8 proteins are highly expressed in liver.

Although the integration of datasets from different levels of systems biology analysis indicates the lack of VX nerve toxin caused significant structural damage on the central nerve system, changes of liver-enriched proteins and inflammatory response-/ acute-phase- associated proteins in serum, clearly suggest the involvement of liver and acute-phase inflammatory processes in VX induced toxicity. Also, the elevated level of mir-133a in serum nicely demonstrates VX-induced damage in muscle tissue.

However, more information is needed to help understand the molecular affects of VX associated toxicity. For example, data from western blots on individual samples from both VX-treatment and control groups will be necessary to confirm these findings. We have been tested a few Abs in VX-treated and control serum samples, but they are all failed due to either the low specificity of Abs, high noise background from serum, or the lower-than detection abundance of target proteins in the blood.

Meanwhile, a list of candidate serum protein/miRNA biomarkers has been unveiled in these systems biological data sets. Many of them may be worth for further validation in blood as potential biomarkers of VX-exposure.

Alternative protein detection methods

Aim 6: Develop new technologies for developing protein-capture agents and the analyses of single protein molecules.

Project Aim 6 called for the development of new protein biomarker discovery methods utilizing surface plasmon resonance (SPR) detection and antibody microarrays, and to apply those methods to the study of *in vivo* and cell culture models of hepatotoxicity. Chris Lausted reports:

Cell culture analyses: In addition to studies summarized (Aims 2,3,4 section C), we attempted to utilize *in vitro* models to study the effects of APAP and additional toxic compounds. Hepatocyte secretions (from HepG2 and other liver cell lines) were analyzed using antibody microarrays which revealed only a very general pattern. The injured cells reduced their secretion of highly-produced proteins such as plasminogen and fibrinogen, but no elevated liver-specific proteins were observed. Cells were treated with toxic levels of amiodarone, nefazodone, tamoxifen and troglitazone as well as non-toxic controls. Our protocol involved the incubation of liver cells for 24 hours in serum-free DMEM, media removal, and 0.2 µm filtration to remove dead cells. The conditional media were concentrated and then diluted in PBS to a final concentration of 100 µg/ml. It appears low levels of expression of cytochrome P450 and of the liver-specific targets in the cell lines were a major limitation with this approach.

Antibody Development: Antibodies are key materials for biomarker research as they are required for microarrays and immunoblots. Furthermore, ELISA assays require pairs of matched antibodies binding to separate protein epitopes. As antibodies were not available for half of our liver-specific targets, we worked to develop a system to produce

high quality monoclonal antibodies and antibody pairs via hybridoma technology. Typically, hybridomas are selected based on an arbitrary level of binding to the target. As we ultimately will require antibodies for use with blood samples, we wish to prioritize the *specificity* of the antibody (where specificity is the difference in affinity for the target protein relative to all other serum proteins).

We have developed a new method to evaluate the specificity of the hybridoma antibodies using a single SPR microarray. The method involves antibody isotyping, quantification, and a set of absolute affinity measurements. The microarray contains antibodies to both IgG and IgM for isotyping. The kinetics of these antibodies are measured once and then used for calculating all of the unknown hybridoma concentrations. The microarray contains a comprehensive collection of liver-specific targets as well as a number of abundant serum proteins, and total human, mouse, and rat serum protein. With the antibody concentrations calculated, the target affinity and the off-target affinities can all be determined in relative or absolute units. The difference between the target affinity and the highest off-target affinity provides the best measure of specificity. The most specific hybridoma antibodies were chosen for full-scale productions. This procedure is both economical and efficient, requiring no labeling and a mere 20 µL of supernatent for quantitative analysis.

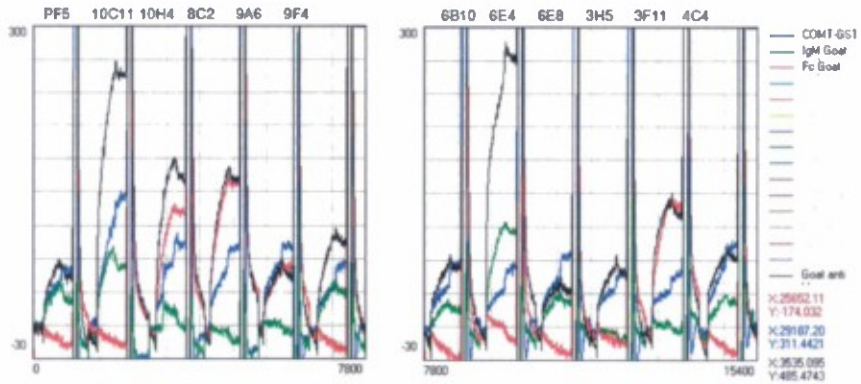

Figure 28. SPR sensorgrams determine the isotype and concentration of antibody in hybridoma supernatants. Twelve hybridoma supernatants raised against a COMT-GST recombinant target all show binding to the target (blue trace). Eight hybridomas contain IgM antibodies (green trace is higher than red trace). Four hybridomas contain IgG antibodies (red trace is higher than green trace). Either the isotype-specific binding (red and green traces), or the isotype independent binding (black trace) may be used to determine hybridoma antibody concentration.

ELISA Development: As biomarkers are of little value without an assay, we worked to develop ELISAs for each candidate biomarker. Using the SPR data, hybridomas were chosen for production based on their suitability for sandwich assays. The resulting antibodies were used to develop conventional chemiluminescent ELISAs. We successfully produced assays for human DPYS, BHMT (capture with monoclonal ISB030-4D1, detection with ProteinTech #212), ALDOB (capture with monoclonal ISB030-5G6, detection with polyclonal), ALDH1L1 (capture with monoclonal ISB030-1C5, detection with polyclonal), PAH (capture with monoclonal ISB030-2A5, detection with polyclonal 036#1), HAO1 (capture with monoclonal ISB030-1F3, detection with polyclonal), MAT1A (capture with monoclonal ISB030-4A3, detection with polyclonal 036#1), and PIPOX (capture with monoclonal ISB030-3A4, detection with polyclonal 036#1),

Linearity always exceeded two orders of magnitude with typical limits of quantitation in the low nanogram per milliliter range using 250 ng of each antibody in the microtitre plate format.

As panels are biomarkers can be more accurate than individual biomarkers, we also worked to develop a multiplexed ELISA to quantify all eight of these liver-specific proteins in addition to a dozen cytokine markers of inflammation. Inflammation in an important factor in drug induced liver injury. We worked to develop a 20-plex protein panel using Nanostring nCounter technology. Intended for RNA measurement, we developed a protein version of the assay with high sensitivity that only requires 5 µL of serum sample. The cytokine portion of the assay was successful, resulting in sensitivity comparably to conventional single-plex ELISAs. Cross-reactivity between the liver-specific proteins was observed, reducing sensitivity to a level inadequate for detecting liver injury. This may indicate that the specificity of our new antibodies is lower than that of the cytokine antibodies used. We will continue to work towards improving and implementing this assay through other sources of funding.

SPR Software: Software was created during the technology development portion of this research has been made public. OSPRAI is the open-source software project at ISB for the analysis of the high-throughput data generated by Surface Plasmon Resonance Imaging. OSPRAI is developed and used by liver toxicity project members, as well as others, for analyzing the antigen arrays used in antibody development and for quantitative proteomics with antibody microarrays. The documentation and code repository is hosted by the servers at the Bioinformatics Organization (http://www.bioinformatics.org/groups/?group_id=1018). This organization hosts bioinformatics collaborations free-of-charge for academic use. Services include software version control (Subversion SVN), bug tracking, forums, and a web page. OSPRAI includes tools for converting common SPR data formats (e.g. Biacore, Lumera, CLAMP, spreadsheets), signal calibration, outlier removal, and kinetic parameter determination by curve-fitting. Prior to this, no such software has been available for SPR microarray analysis.

Publications: Quantitative serum proteomics from surface plasmon resonance imaging."
Christopher Lausted, Zhiyuan Hu, and Leroy Hood. Mol Cell Proteomics. 2008 Dec;7(12):2464-74.

Efficient antibody screening using surface plasmon resonance imaging of antigen microarrays." Christopher Lausted, Zhiyuan Hu, and Leroy Hood. In preparation.

O Name and telephone number of preparer of the report

Lee Rowen, 206-732-1272 and Trudy Adkins, 206-732-1222